

Introduction to Small-Angle Scattering

SAXS & ASAXS



Dr. Armin Hoell

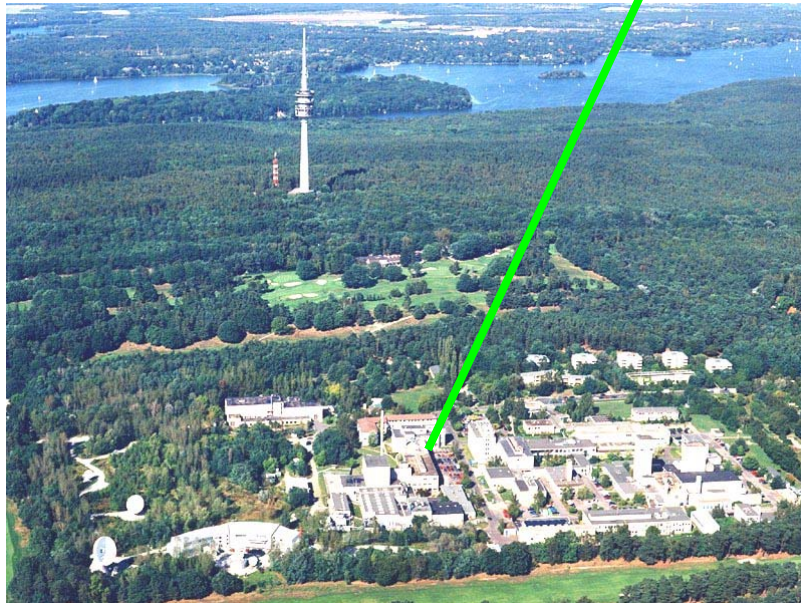


Lecture series: Modern Methods in heterogeneous catalysis research: FHI, WS 2014-2015

Liese-Meitner-Campus Wannsee
-Neutron reaktor as neutron source:
BER II
-solarenergie research



Wilhelm-Conrad-Roentgen Campus
Adlershof
-Synchrotron source: BESSY II
-solarenergie research



Introduction SAS:

- some historical remarks
- when can small-angle scattering be used
- kind of samples

Small-Angle Scattering:

- scattering vector, size range to be investigated
- theoretical remarks
- structural parameters, the scattering contrast
- Which are possible structural results of SAS

Model scattering curves:

Example of instrumentation: **-ASAXS instrument at BESSY II**

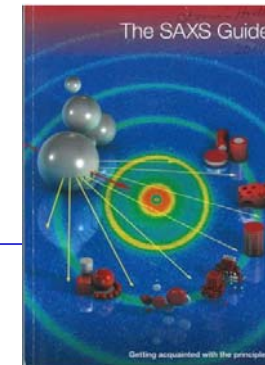
Contrast variation:

-ASAXS; resonant Small-Angle X-ray Scattering

Examples:

- RuSe – catalyst for fuel cells
- degradation of PtNi₃ catalysts studied by ASAXS

Heimo Schnablegger: „**The SAXS Guide**“ Firma Anton Paar, Austria
online available from institute ILL / Grenoble in France



Guinier (1956/1994) “X-ray diffraction. In crystals, imperfect crystals, and amorphous bodies”, Chapter 10 Small-angle x-ray scattering.

Glatter & Kratky (ed.) (1982) “Small Angle X-ray Scattering”. (<http://physchem.kfunigraz.ac.at/sm/Software.htm>)

Feigin & Svergun (1987) “Structure analysis by small-angle X-ray and neutron scattering”, (http://www.embl-hamburg.de/ExternalInfo/Research/Sax/reprints/feigin_svergun_1987.pdf)

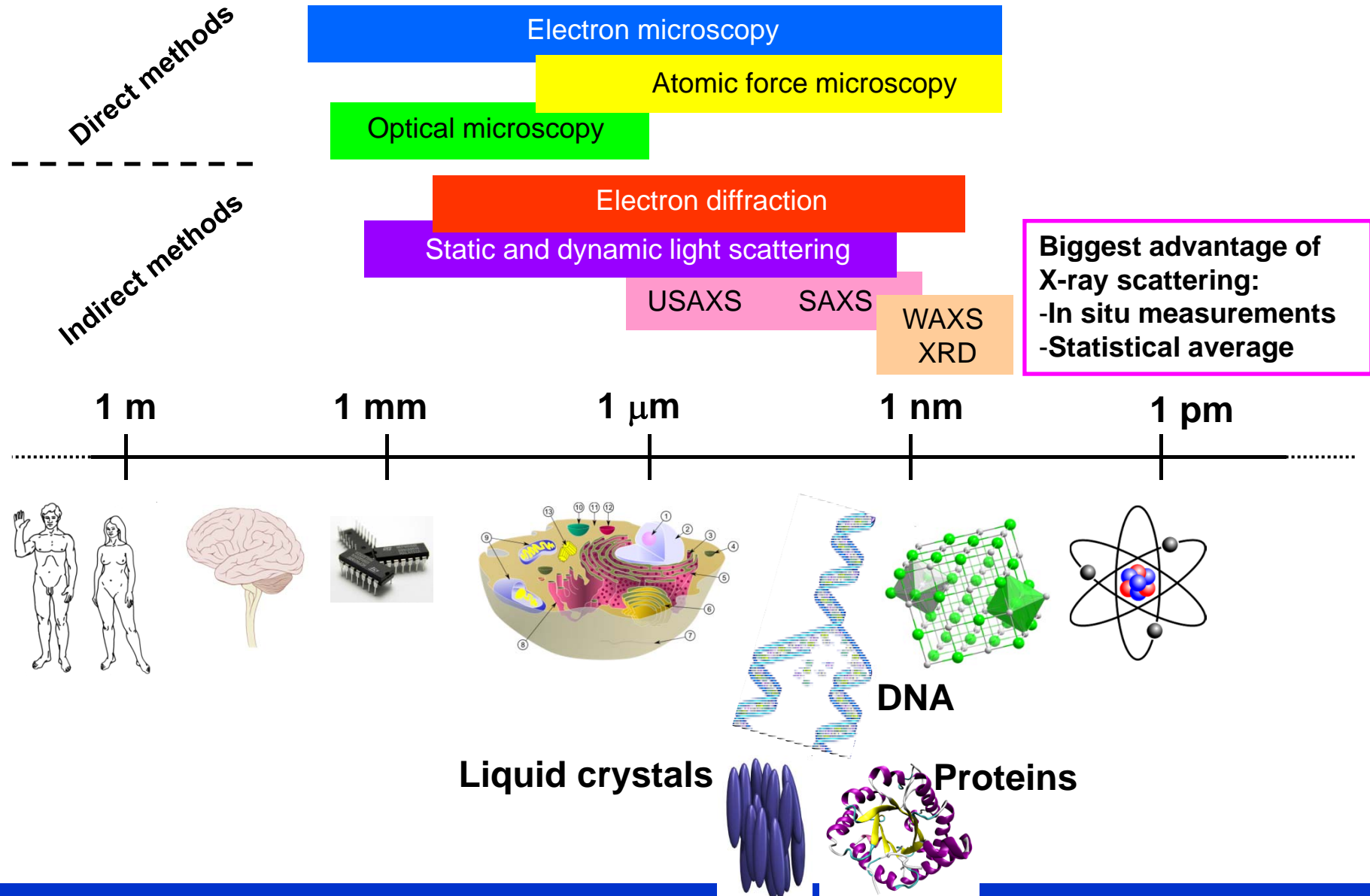
Guinier & Fournet, (1955), “Small-angle scattering of X-rays”, New York

Otto Kratky (1983) “Die Welt der vernachlässigten Dimensionen und die Kleinwinkelstreuung der Röntgen-Strahlen und Neutronen an biologischen Makromolekülen”, Nova Acta Leopoldina, Halle.

27. IFF-Ferienkurs (1996) “Streumethoden zur Untersuchung kondensierter Materie”, Jülich.
ISBN 3-89336-180-4

Software to analyse the Small-Angle Scattering curves. **SASFIT** / Joachim Kohlbrecher: PSI
<https://kur.web.psi.ch/sans1/SANSSoft/sasfit.html>

Structural determination of different materials



History: SAXS and Anomalous SAXS

1930 Krishnamurti, P. *Indian J. Phys.*, 5, 473–500 (1930). “Studies in X-Ray Diffraction. Part I: The Structure of Amorphous Scattering. Part II: Colloidal Solutions and Liquid Mixtures.” Particle size and molecular weights related to extent of small-angle scattering.

1940 – 1960 – Guinier, Debye, Luzatti, Porod and others develop interpretation for the basic features in SAXS patterns

1980 Stuhrmann (EMBL Hamburg; instrument X15) **first ASAXS** or Ferritin and Hemoglobin

J.P. Simon; O. Lyon; France A. Bienenstock; Stanford, USA
ASAXS on alloys and theory

HASYLAB JUSIFA instrument at B1 (Haubold; FZ Juelich)

1991 ASAXS at A1 (lower energy range, organic materials) Stuhrmann

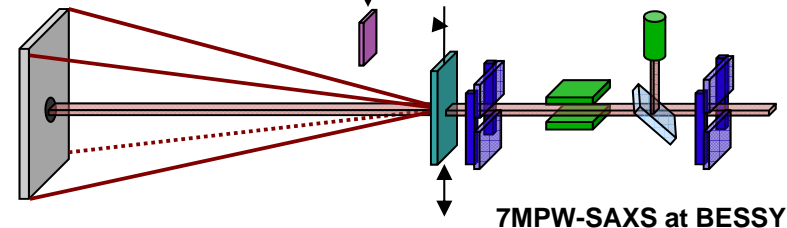
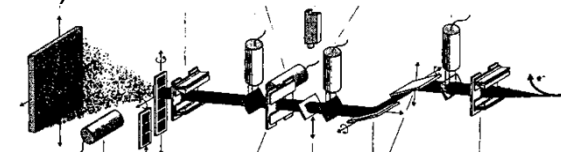
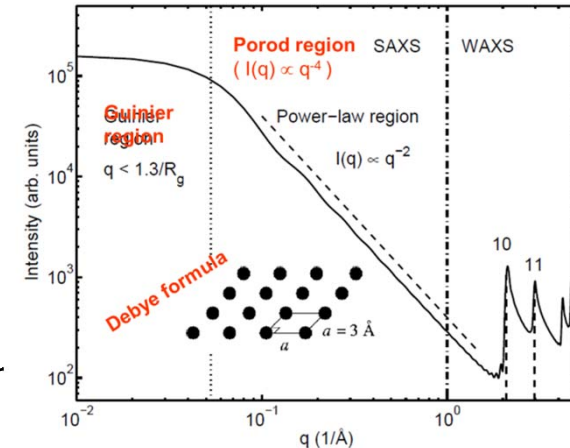
No real dedicated ASAXS instruments furthermore:
ID01 & BM02 @ ESRF; 12ID at APS

HMI - SAXS instrument at BESSY: dedicated to anomalous and grazing incidence SAXS

3/2006

Our goals:

- Application of ASAXS in the material science field and materials for renewable energy sources
- Increase the sensitivity and accuracy of ASAXS
- Further development of ASAXS theory



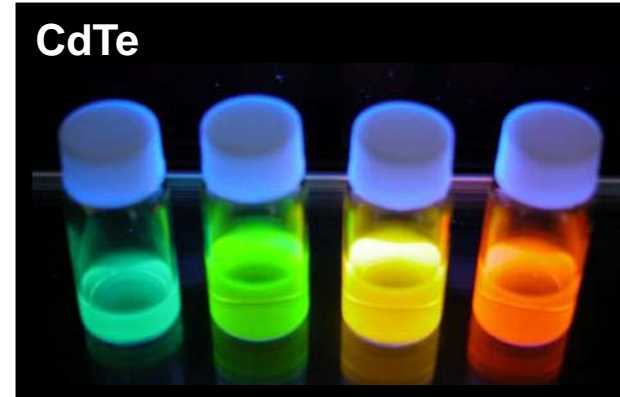
7MPW-SAXS at BESSY

**-in general all nanostructures containing materials
(in state of solid plates, powders, or liquids)**

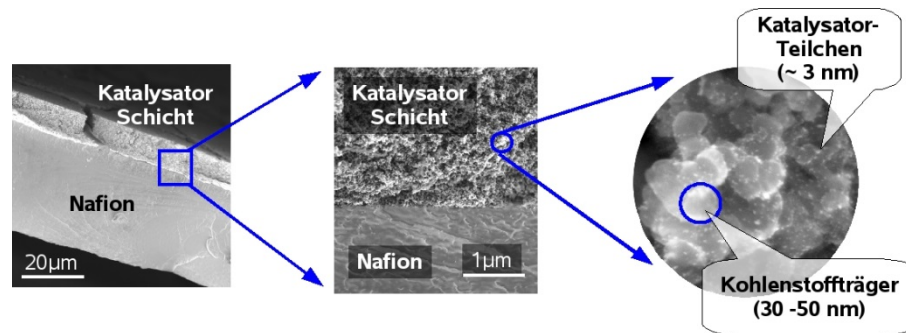
Examples:

- immiscibility regions and beginning crystallization in e.g. glasses
- precipitations in alloys
- concentrations fluctuations at phase boundaries (e.g. hydrogen storage)
- grain boundaries in polycrystalline materials
- pore structures in aero gels, porous glasses ...
- morphology of biological cells, DNS, bones, woods
- polymers
- colloidal liquids: protein structures, magnetic fluids
- catalysts; especially nonoparticles on different supports

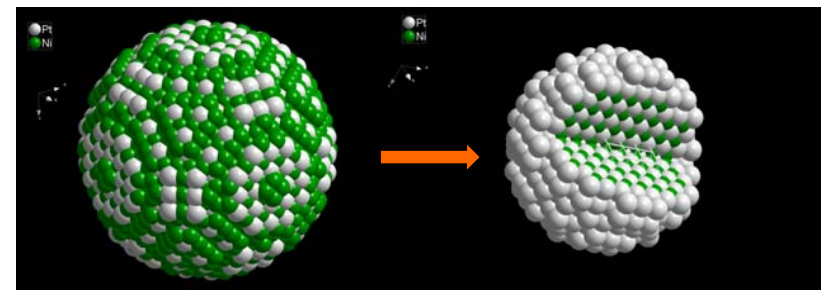
Luminescent Nano- crystals:



Different catalysts:



PtNi_3



Historical Gold-Ruby Glass: old roman *Lycurgus cup*

nature photonics | VOL 1 | APRIL 2007 | www.nature.com/naturephotonics

OPTICAL METAMATERIALS

Invisibility cup

Ulf Leonhardt

Cloaking devices for visible light come a step closer to reality by combining the modern form of a Roman technology with ideas from ancient Greece.

Ulf Leonhardt

is in the School of Physics and Astronomy,
University of St Andrews, North Haugh, St Andrews,
KY16 9SS, UK.

e-mail: ulf@st-and.ac.uk

One of the things the Romans did for us was the invention of the first optical metamaterial — ruby glass. They probably did not know it, but their recipe for ruby glass contained one crucial ingredient: tiny gold droplets, typically 5–60 nm in size. These gold particles colour the glass in an extraordinary way, as demonstrated by the exquisite Lycurgus Cup (Fig. 1). In daylight the cup appears a greenish colour, but illuminate it from the inside and it glows ruby. On page 224 of this issue, Cai *et al.* present theoretical simulations that show that a modified Roman cup based on modern nanofabrication technology will act as an invisibility device, albeit for one polarization and one specific colour of light. Any object you put inside will

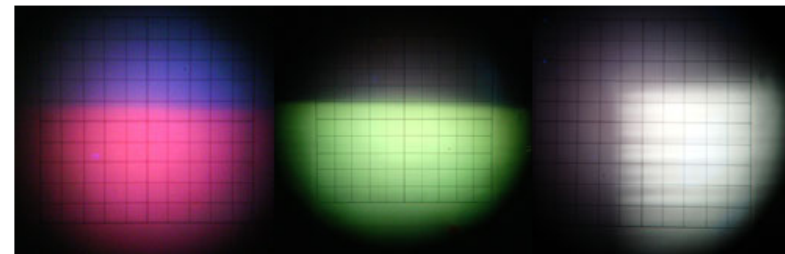


Lumineszierende Gläser

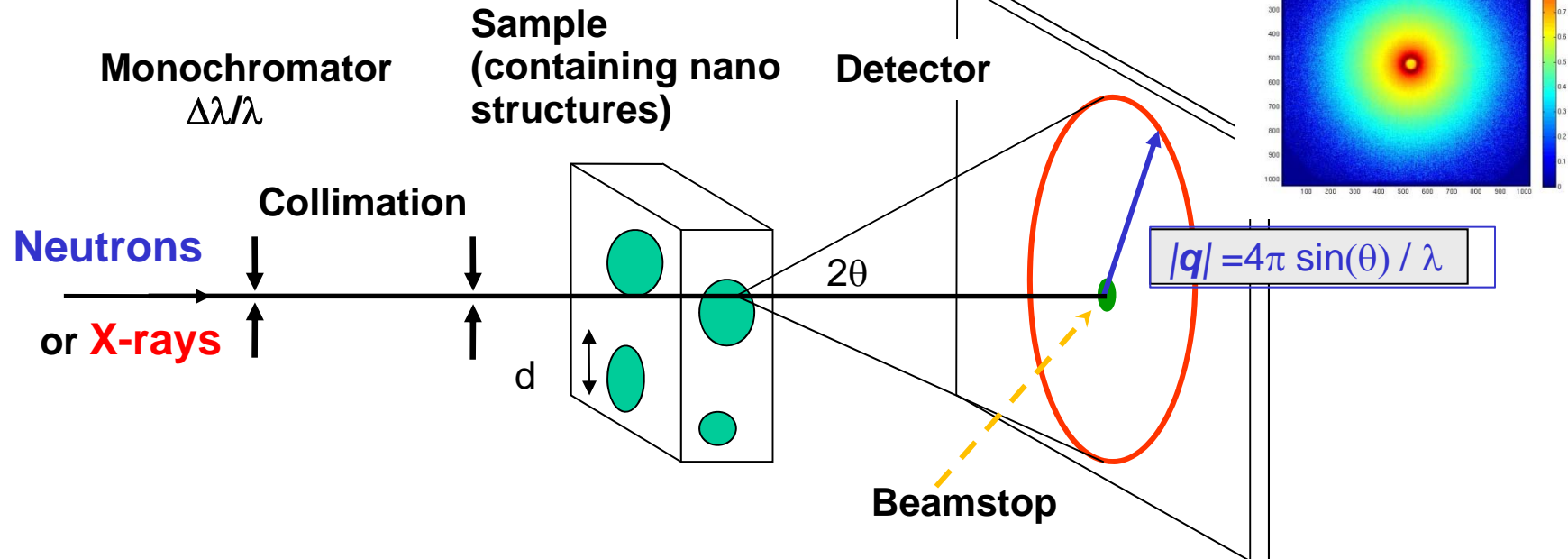
DOI: 10.1002/anie.200123456

Intensive rote, grüne und weiße Lumineszenz in photoaktivierten gold- und silberhaltigen Silicatgläsern**

Maik Eichelbaum, Klaus Rademann, Wilfried Weigel, Armin Hoell, Dragomir M. Tatchev*



Principle of Small-Angle Scattering (SAS)



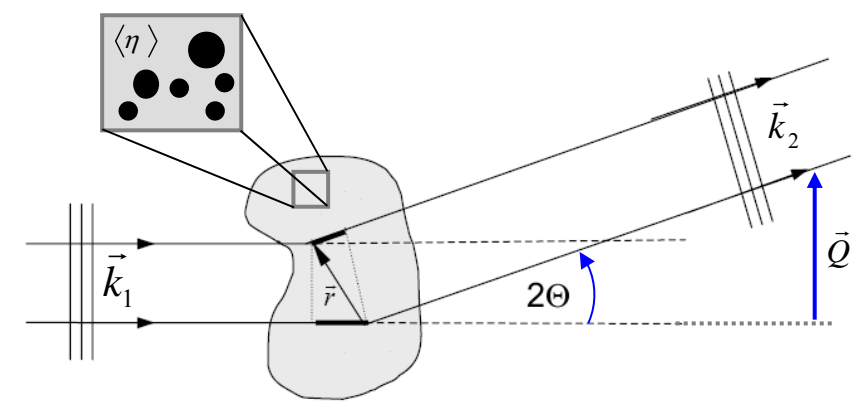
Inhomogeneity of densities, composition fluctuations and magnetisation in size ranges of d : $\sim 0.5 - 100$ nm

One can get: Size distributions, distances, compositions, volume fractions

Intensity $I(q)$ $q = 2\pi/d$
Scattering angle 2θ : $0.1 - 6^\circ$

important: sample properties

Scattering cross-section



Scattering vector: $\vec{Q} = \vec{k}_2 - \vec{k}_1$

Resolution limit: $r_{\min} = \frac{\pi}{Q_{\max}}$

SAS range: $0 \leq Q \leq \frac{\pi}{d_A}$

⇒ Colloidal dimensions: $\sim 1 - 100 \text{ nm}$

Material:
that contains
nanostructures

How can colloidal structures be investigated?

Magnitude of the scattering vector

$$|\vec{q}| = \frac{4\pi \sin(\theta)}{\lambda}$$

Bragg-equation

$$2d \sin(\theta) = \lambda$$

$$|\vec{q}| = \frac{2\pi}{d}$$

Threshold
value:

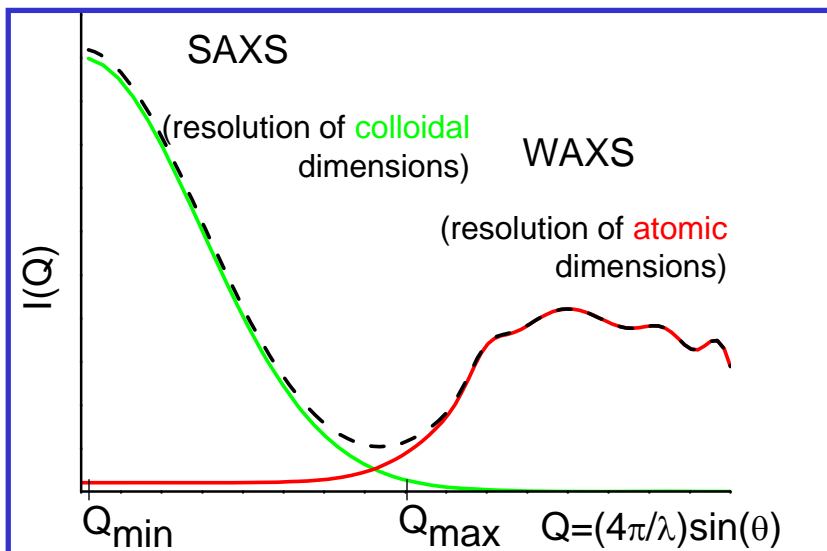
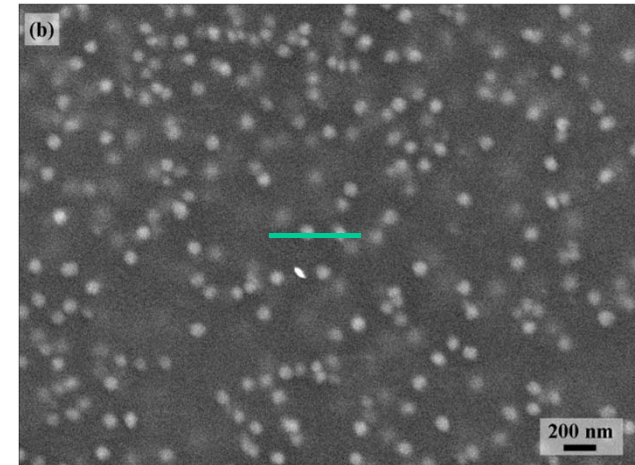
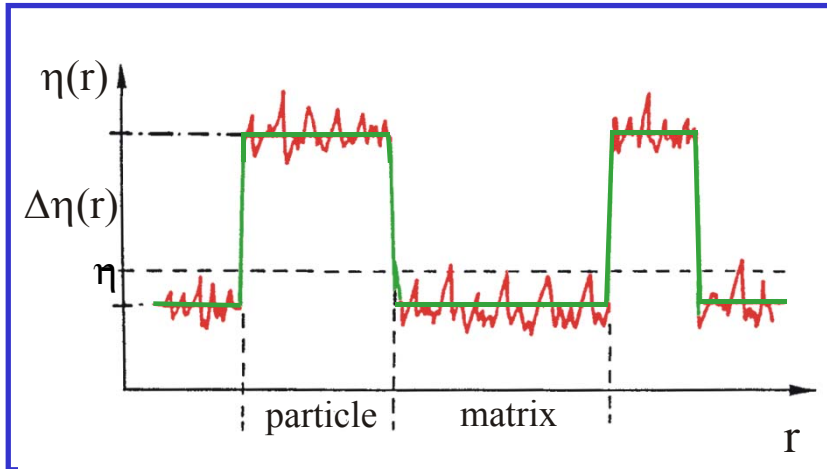
$$|\vec{q}| \rightarrow 0$$

$$d \rightarrow \infty$$

Scattering also allows to investigate structures in the nm- and μm - range.

→ Small-Angle Scattering (SAXS, SANS, USAXS, USANS) ←

Inhomogeneities of scattering length density, η , [introduction scattering length density later]
in a size range of: $\sim 0.5 - 200$ nm

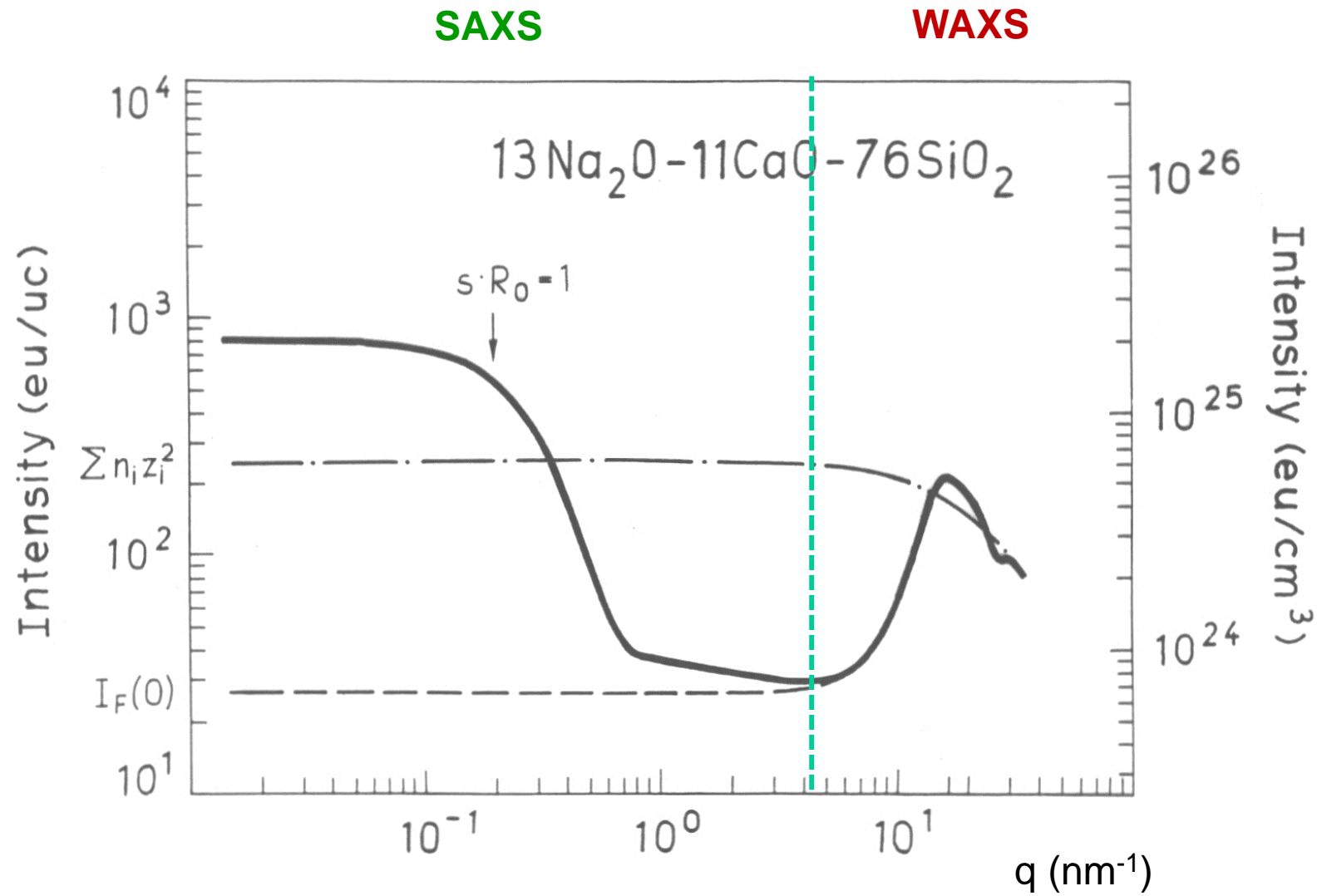


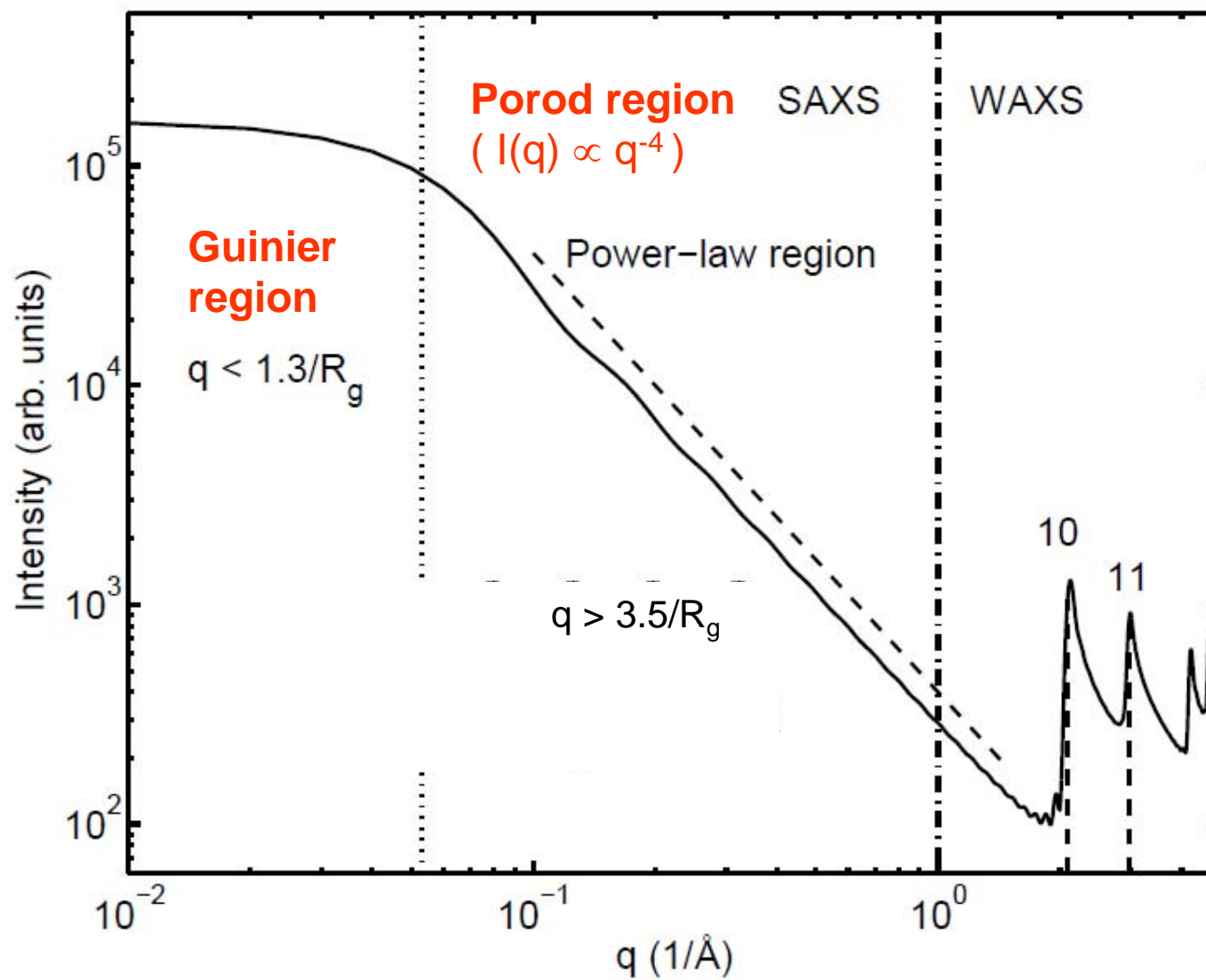
Resolution limit: $r_{\min} = \frac{\pi}{Q_{\max}}$

View field limit: $r_{\max} = \frac{\pi}{Q_{\min}}$

SAS does not have resolution for interatomic distances.

Therefore, SAS alone can not distinguish whether a nanostructure is crystalline or amorphous.





Scattering Intensity:

$$I(Q) = N_V (\Delta\rho)^2 V^2 F(Q, R)^2$$

Scattering Amplitude of a sphere of radius R:

A

Guinier region: for $Q \Rightarrow 0$

$$I(Q) = I(0) \exp(-R_0^2 Q^2 / 3)$$

$$R_0^2 = -3 \lim_{Q \rightarrow 0} \left[\frac{d \ln(I(Q))}{d(Q^2)} \right]$$

R_0 : radius of gyration

Fluctuations of electron density:

$$\Delta\rho(r) = \rho(r) - \bar{\rho}$$

$$F(Q, R) = 3 \frac{\sin(QR) - QR \cos(QR)}{(QR)^3}$$

B

Porod region: for large Q

$$I(Q) \approx K_1 / Q^4$$

$$K_1 = \lim_{Q \rightarrow \infty} [Q^4 I(Q)] = 2\pi (\Delta\rho)^2 S_V$$

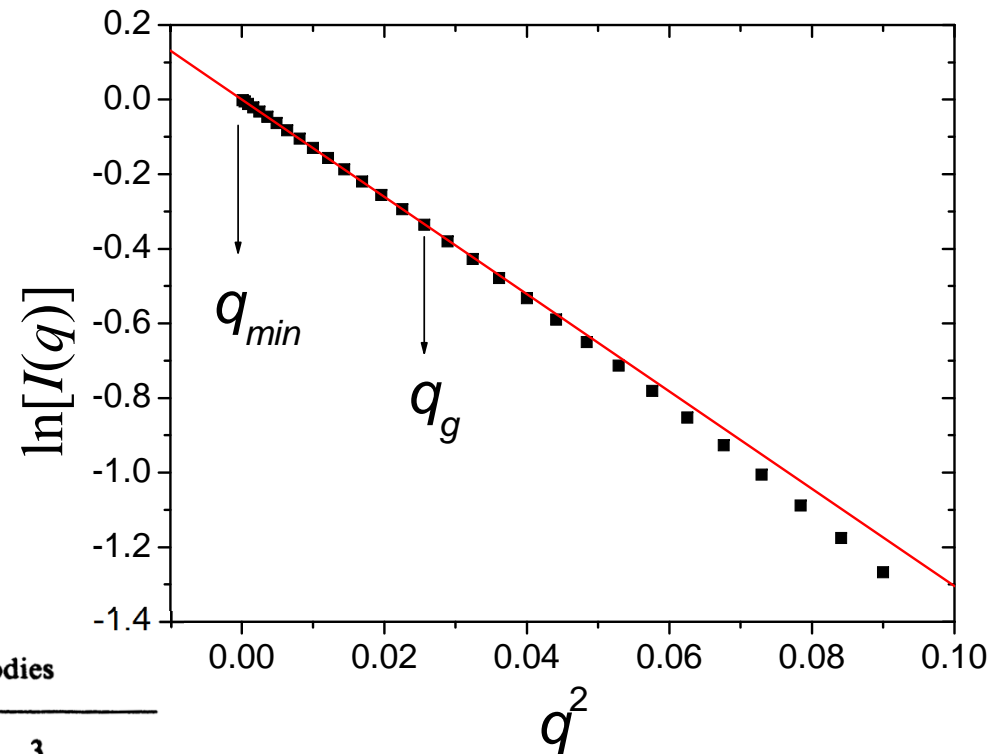
S_V : interphase surface area

Approximation at **small** q

$$q \rightarrow 0; \quad R_g q_g < 1$$

$$I(q) = I(0) \exp(-q^2 R_g^2 / 3)$$

$$R_g = \sqrt{\frac{\int_V \Delta\rho(\vec{r}) r d\vec{r}}{\int_V \Delta\rho(\vec{r}) d\vec{r}}}$$



Guinier plot

$$\ln[I(q)] = \ln[I(0)] - (R_g^2 / 3) q^2$$

Table 3.1. Radii of Gyration of Some Homogeneous Bodies

Sphere of radius R

$$R_g^2 = \frac{3}{5} R^2$$

Spherical shell with radii $R_1 > R_2$

$$R_g^2 = \frac{3 R_1^5 - R_2^5}{5 R_1^3 - R_2^3}$$

Ellipse with semiaxes a and b

$$R_g^2 = \frac{a^2 + b^2}{4}$$

Ellipsoid with semiaxes a , b , and c

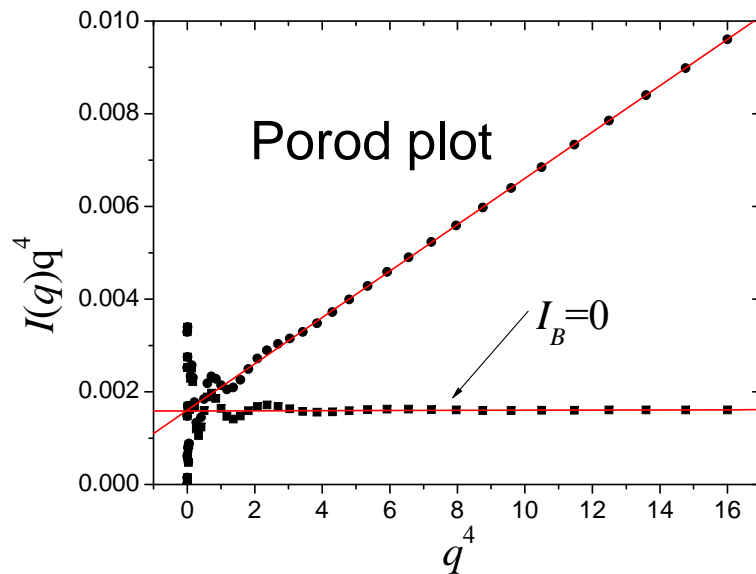
$$R_g^2 = \frac{a^2 + b^2 + c^2}{5}$$

Approximation at **large** q $q \rightarrow \infty$

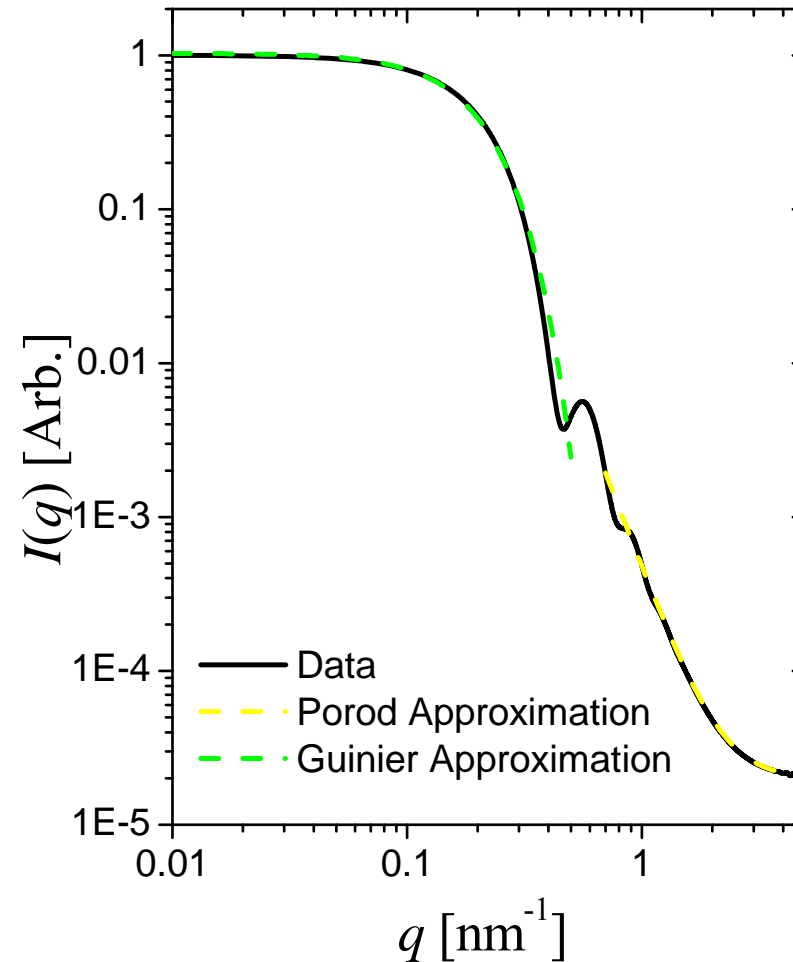
$$I(q) \approx K_P / q^4 \quad I(q) \approx \tilde{K}_P / q^3$$

$$I(q) \approx K_P / q^n + I_B$$

$$K_P = 2\pi(\Delta\rho)^2 S$$



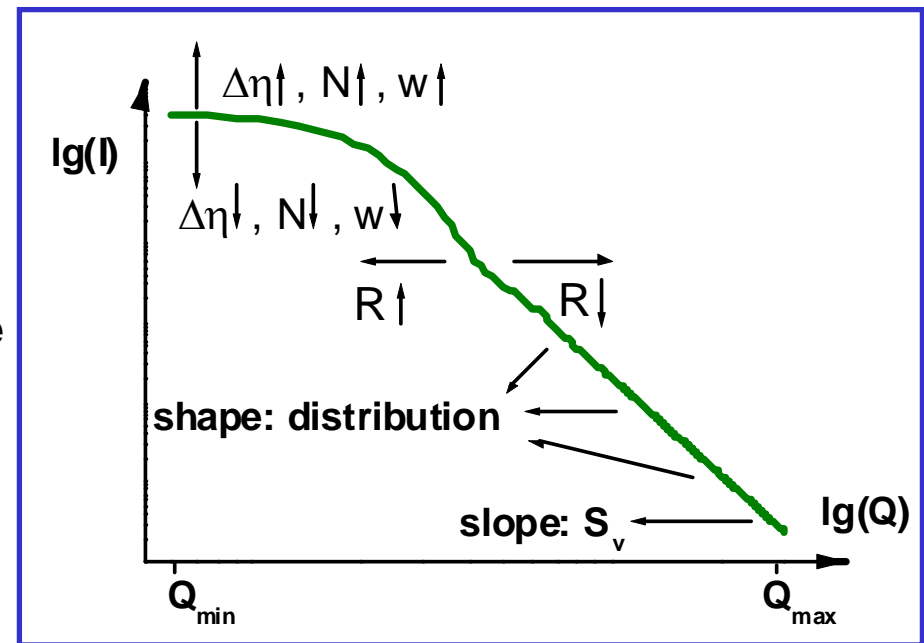
$$I(q)q^n \approx K_P + I_B q^n$$



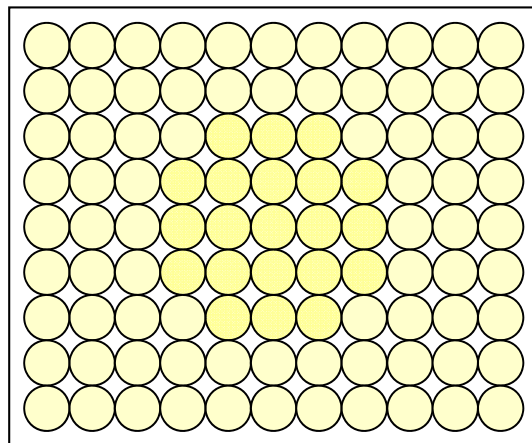
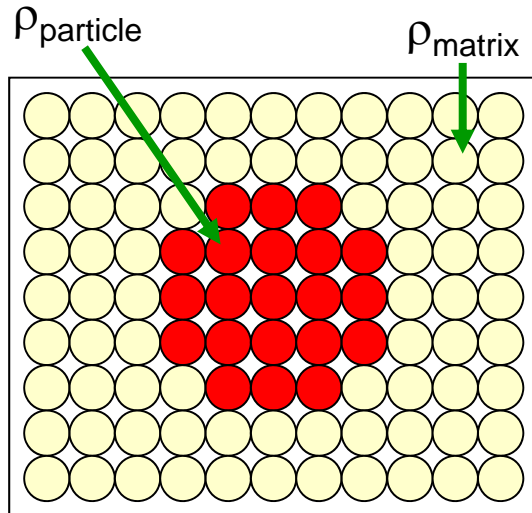
K_P – proportional to the interphase surface area

$$I(Q) = N_p \int \{\Delta\eta V_p(R) F(QR)\}^2 S(QR_{hc}) N(R) dR$$

\downarrow \downarrow \downarrow \downarrow
Contrast: $\Delta\eta = \eta_{\text{particle}} - \eta_{\text{matrix}}$ **Particle shape factor** **Inter-particle interference** **Size distribution**



electron density:



$$\rho = \frac{N_A D \sum_i c_i z_i}{M_C}$$

Electron density: $\rho(r)$

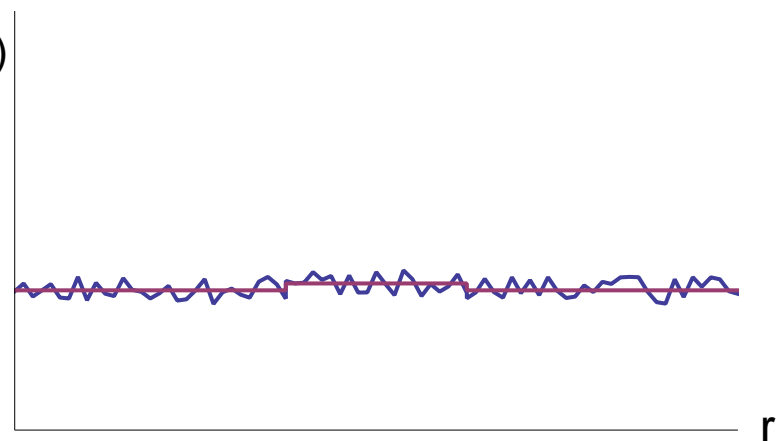
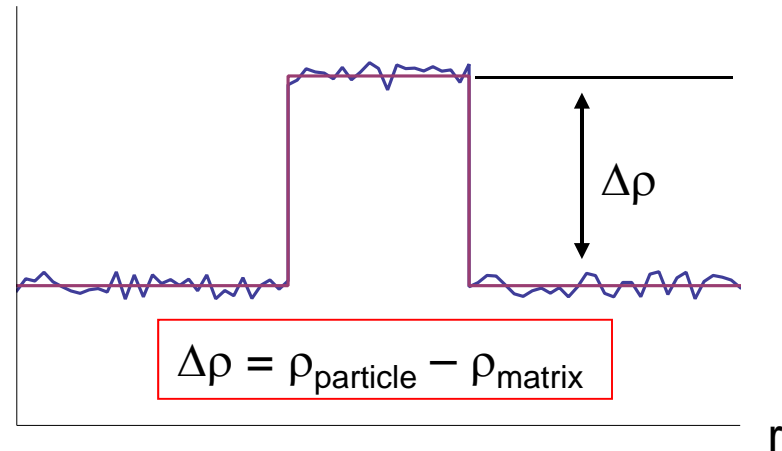
$$(\Delta\rho)^2 > 0$$

Electron density : $\rho(r)$

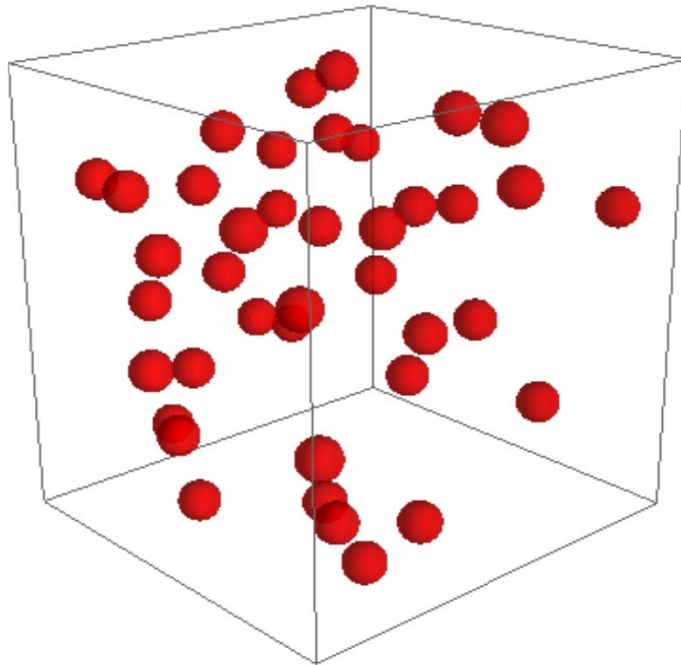
$$(\Delta\rho)^2 \cong 0$$

general:

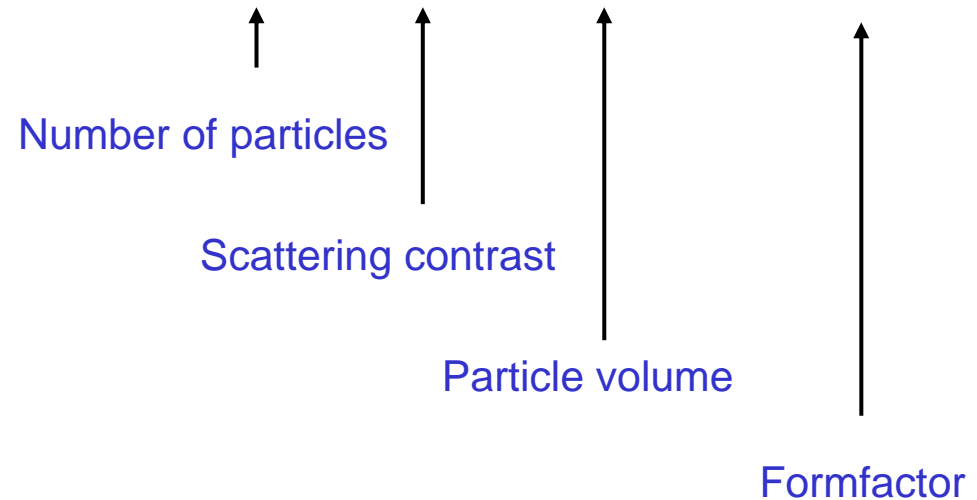
Scattering length density



Case 1: Monodisperse spherical particles in a solution (matrix)



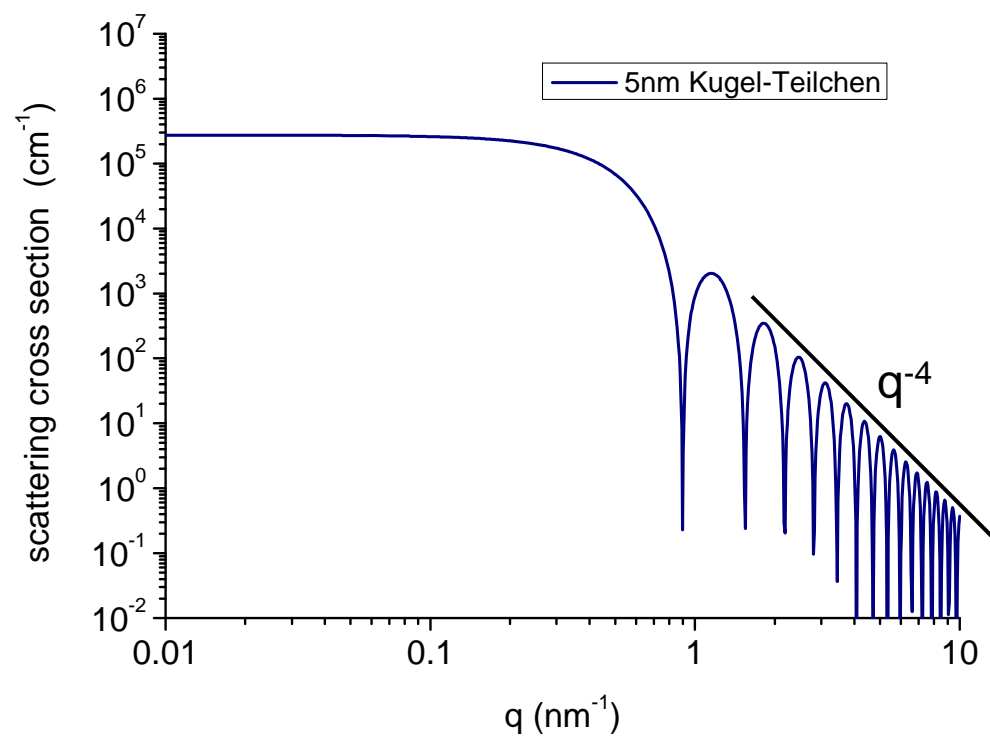
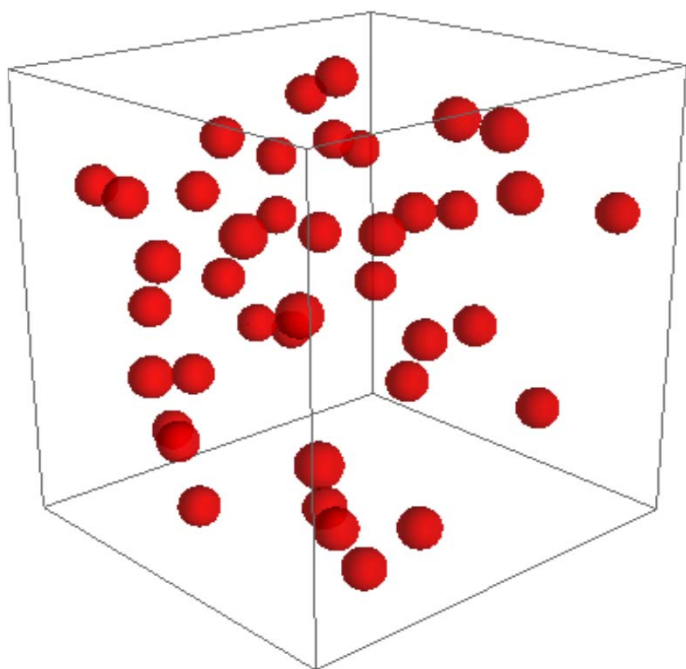
$$I(q) = N_P \times (\Delta\rho)^2 \times V_P^2(R) \times F^2(q, R)$$



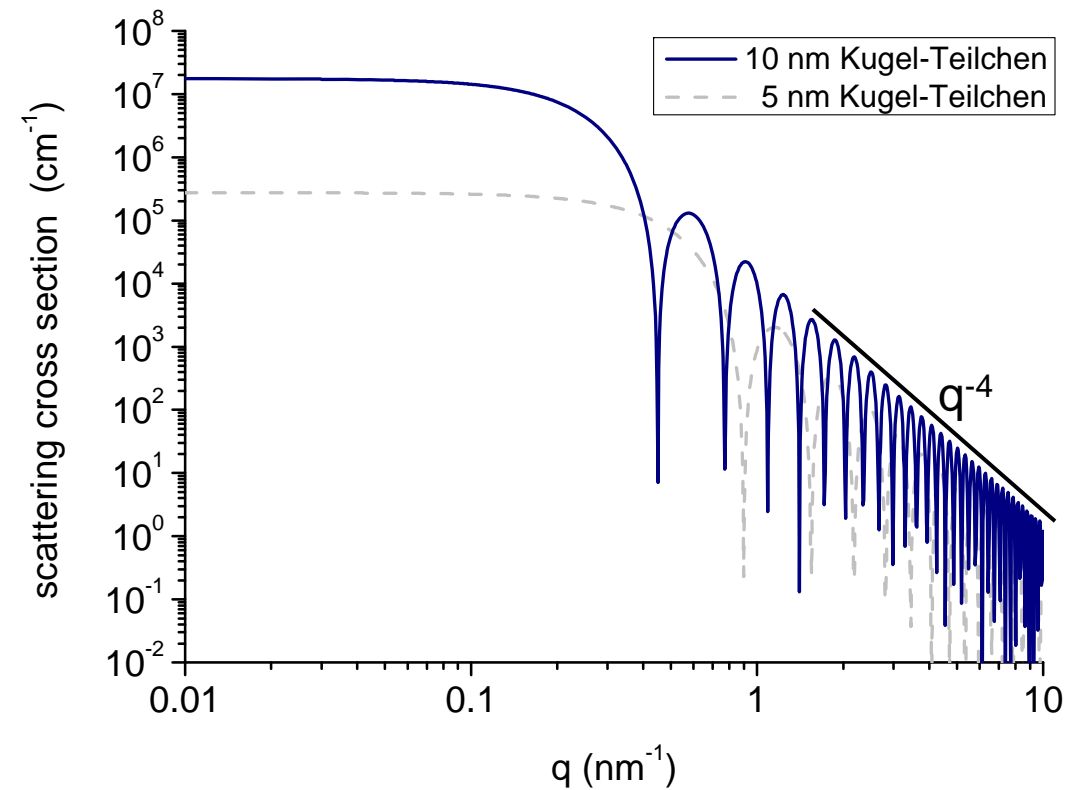
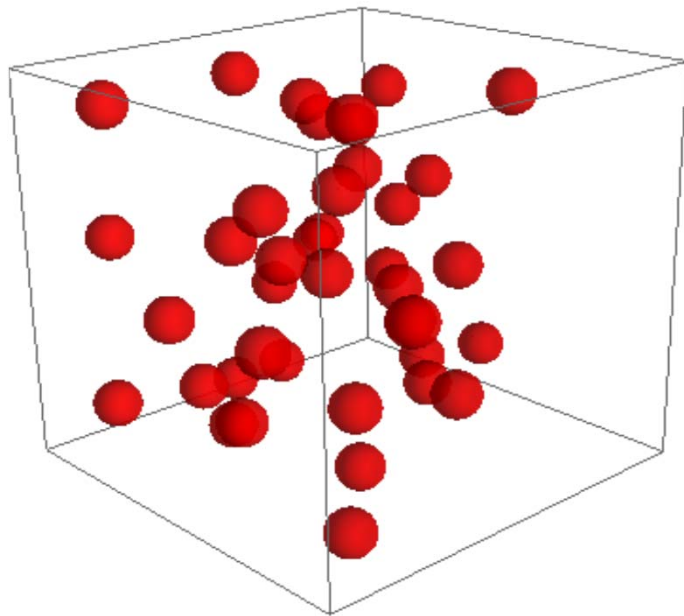
Scattering amplitude of a homogeneous sphere:

$$F(Q, R) = 3 \frac{\sin(QR) - QR \cos(QR)}{(QR)^3}$$

Case 1: Monodisperse spherical particles in a solution (matrix)

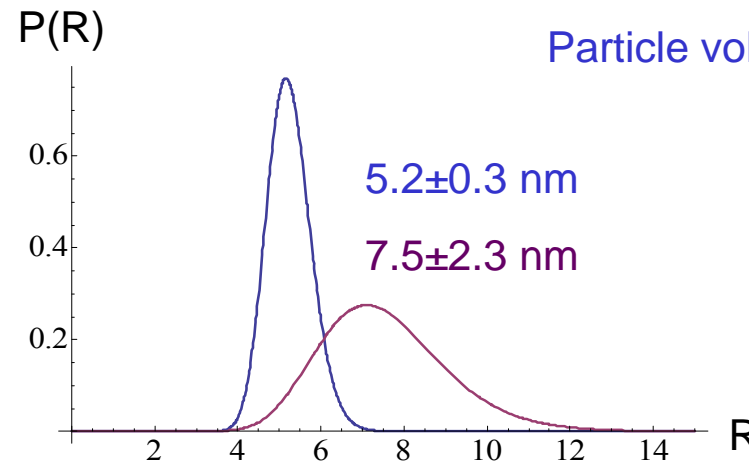
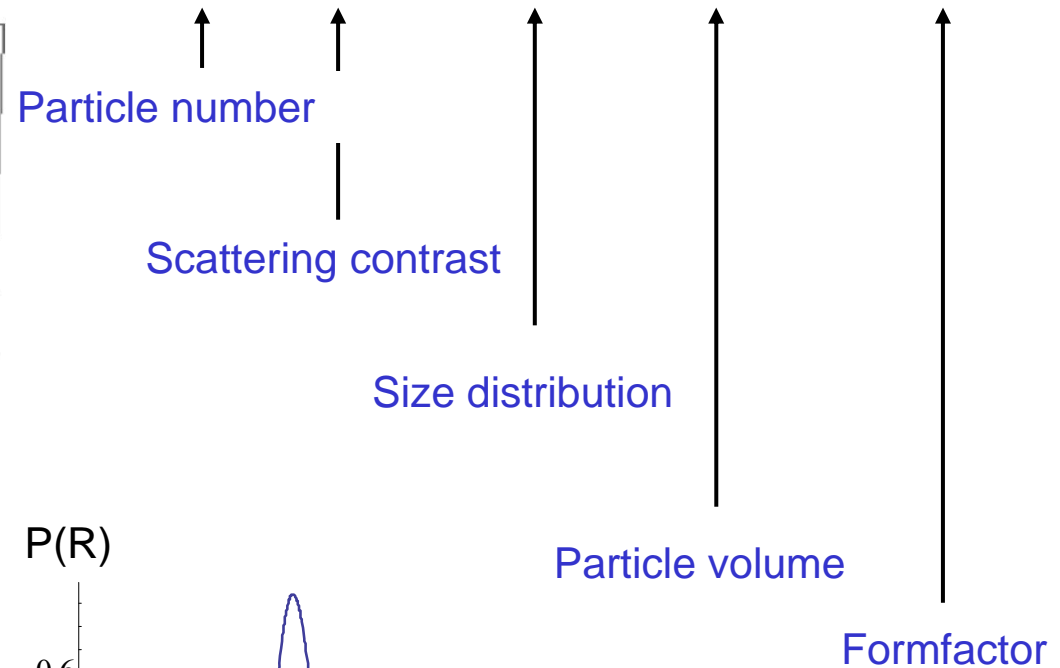
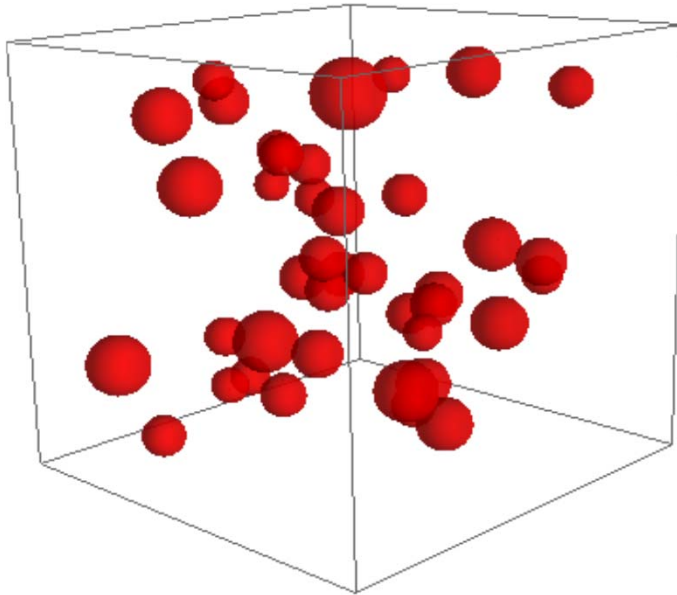


Case 1: Monodisperse spherical particles in a solution (matrix)

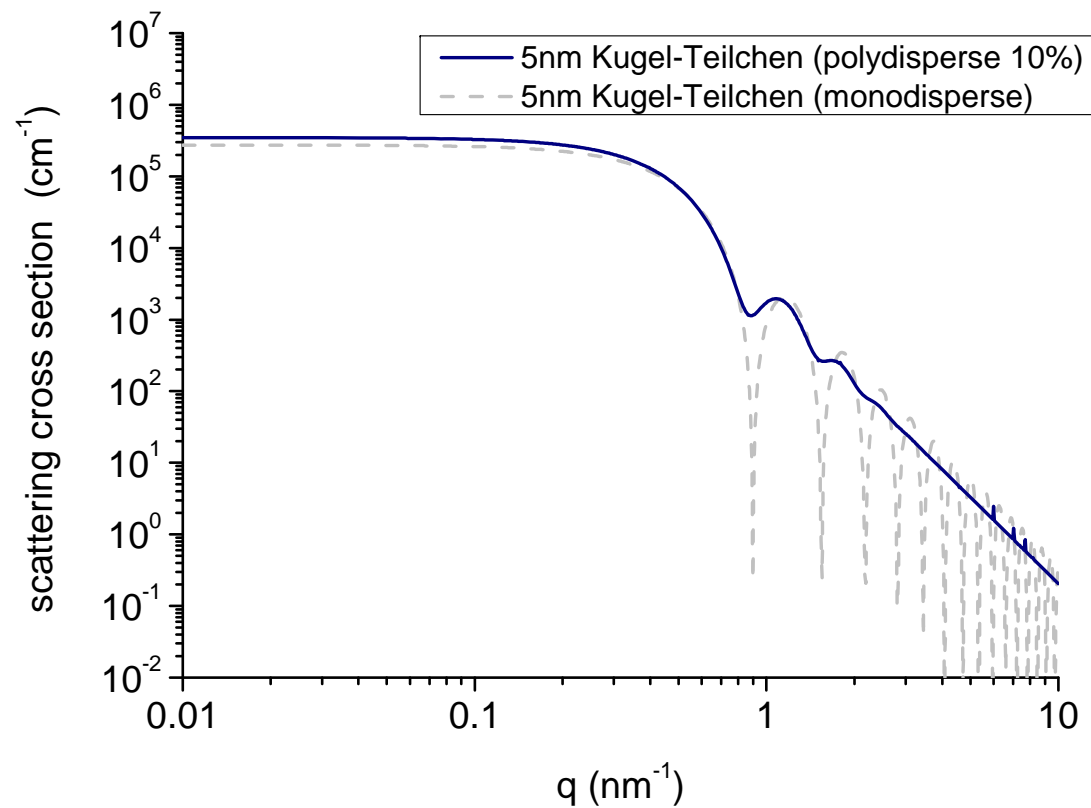
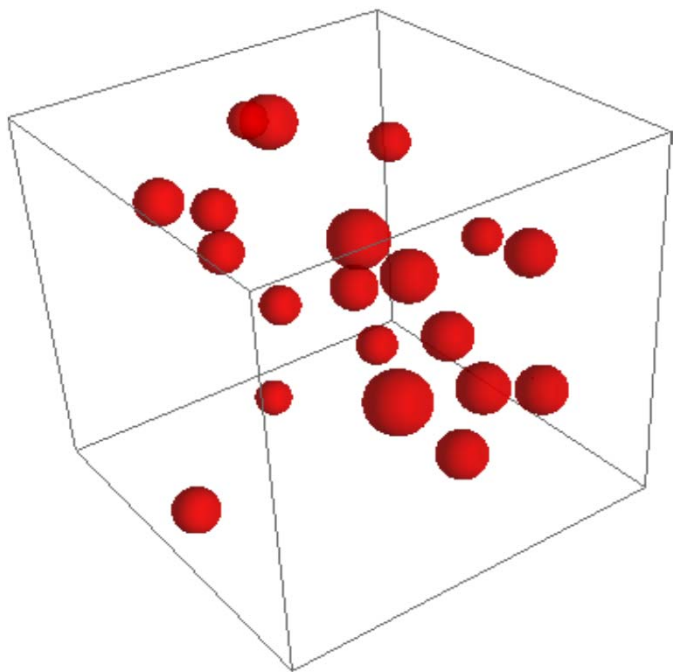


Case 2: Polydisperse spherical particles in a solution (matrix) (diluted system)

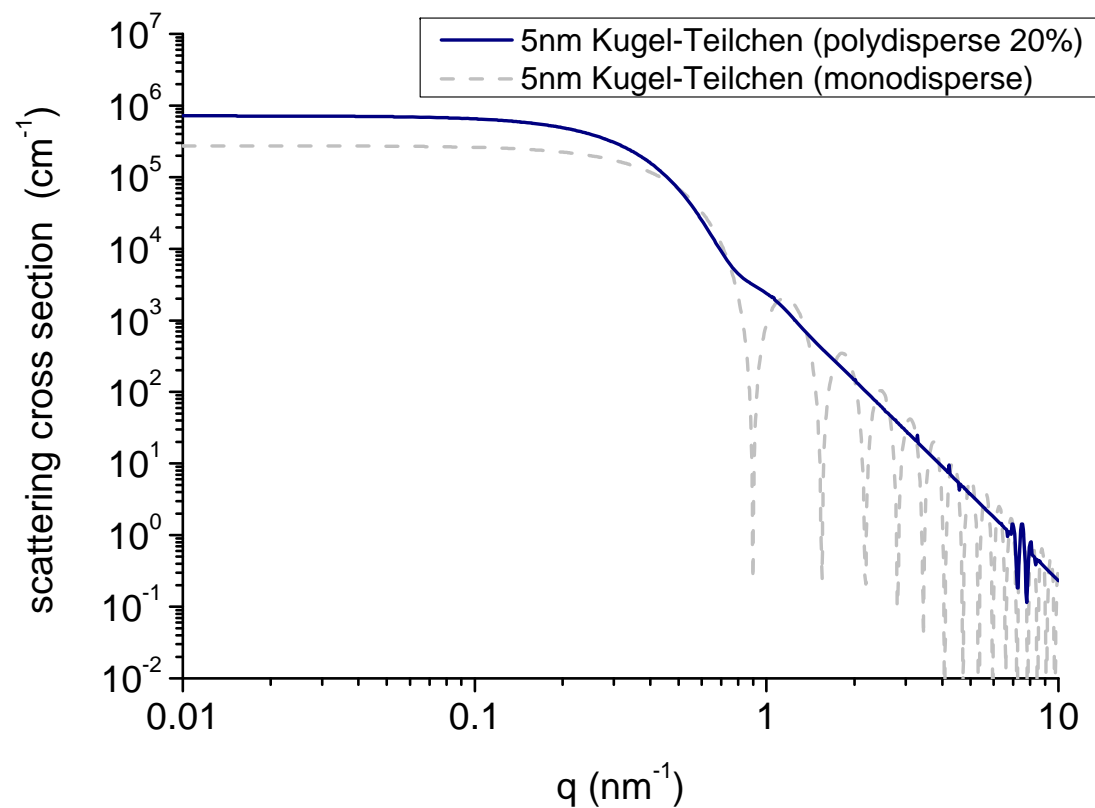
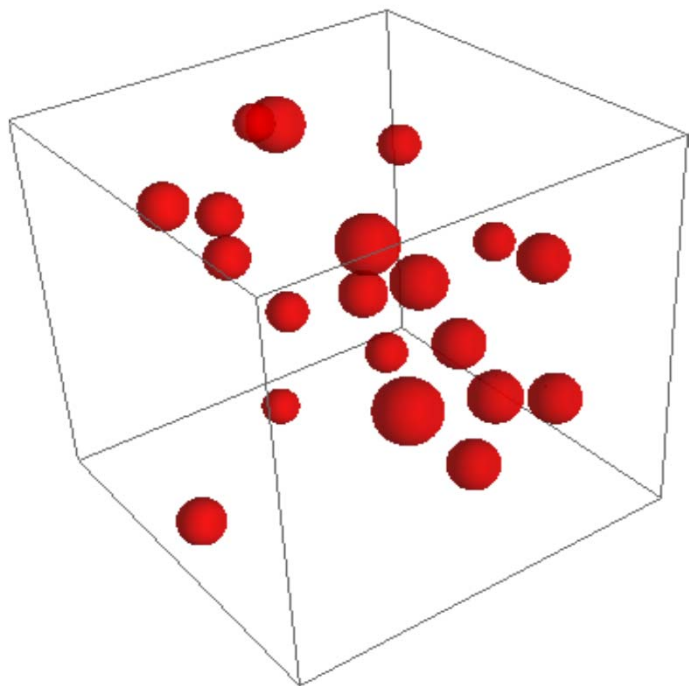
$$I(q) = N_p \times (\Delta\rho)^2 \times \int P(\tilde{R}) \times V_p^2(\tilde{R}) \times F^2(q, \tilde{R}) d\tilde{R}$$



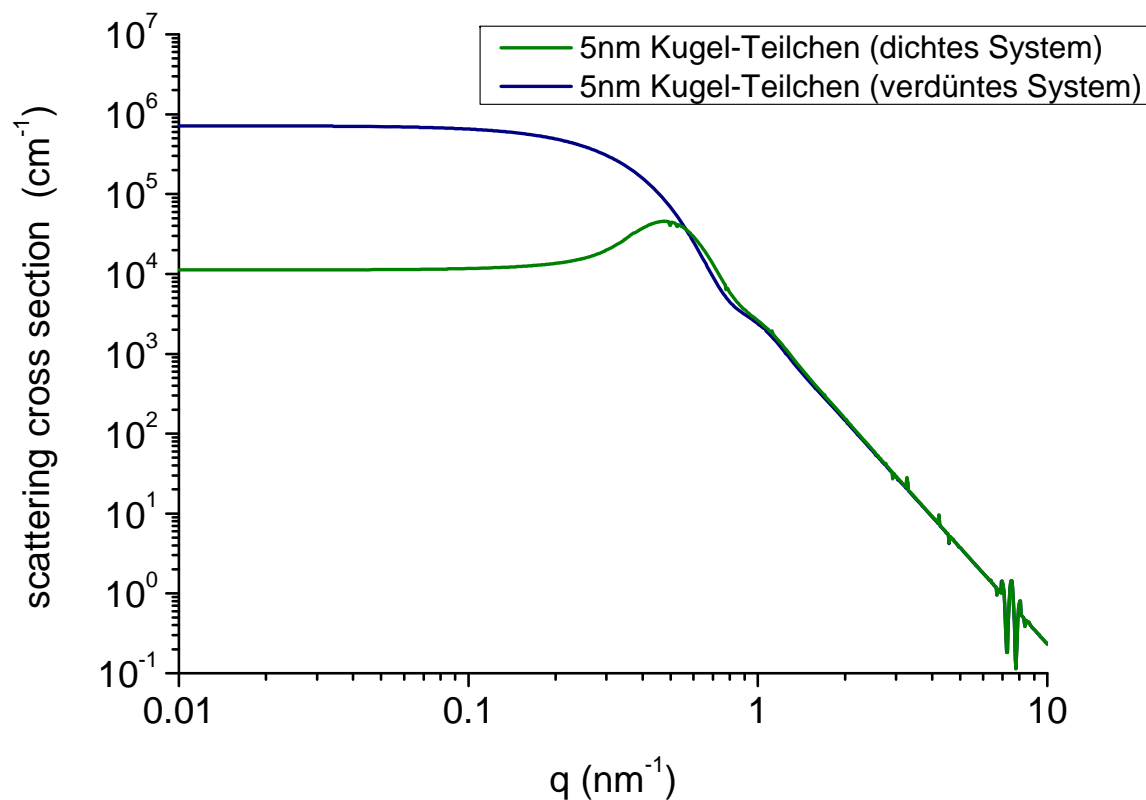
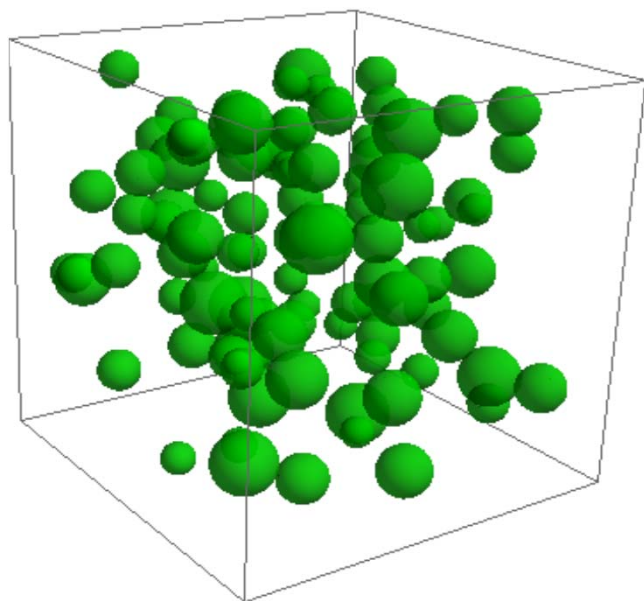
Case 2: Polydisperse spherical particles in a solution (matrix) (diluted system)



Case 2: Polydisperse spherical particles in a solution (matrix) (diluted system)

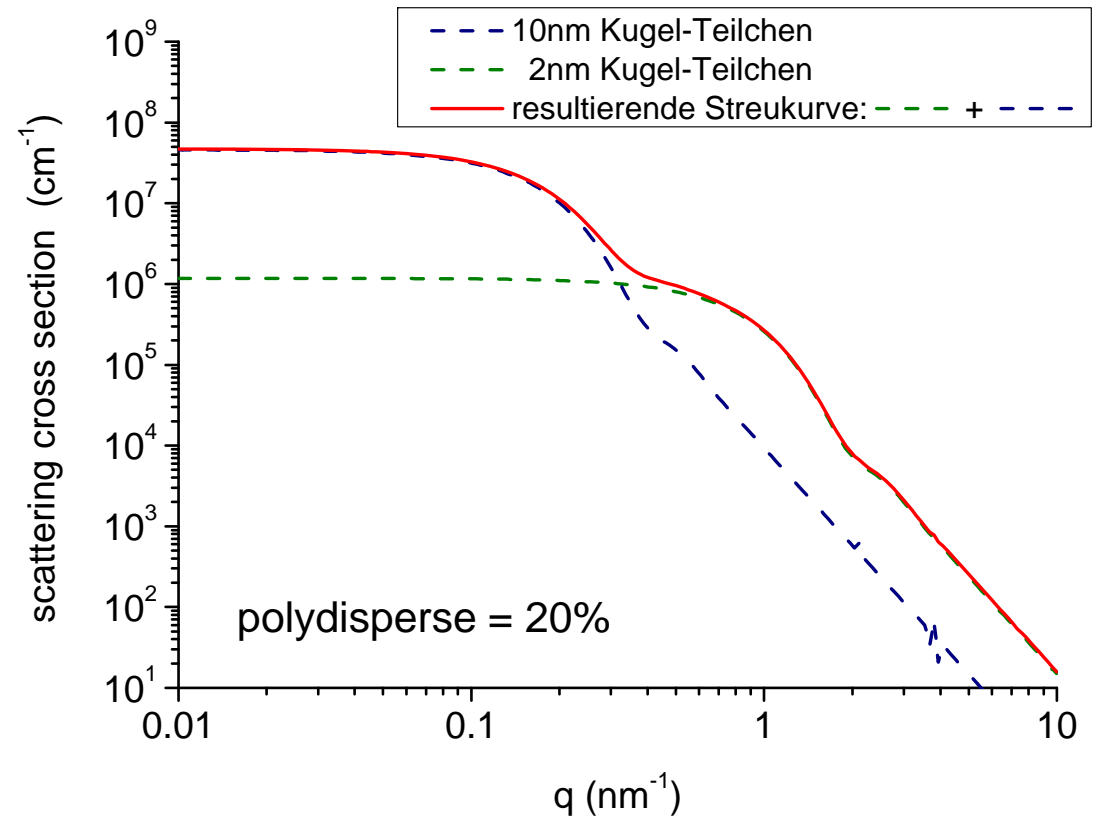
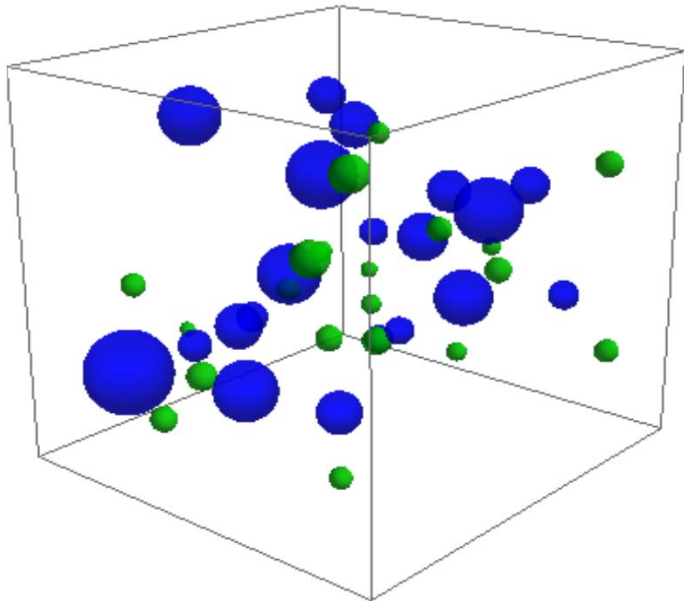


Case 3: Polydisperse spherical particles in a solution (matrix) (dense system)



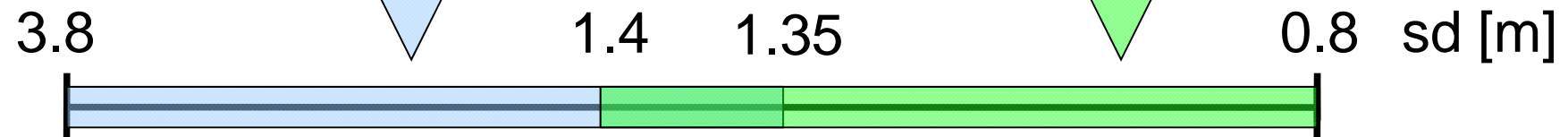
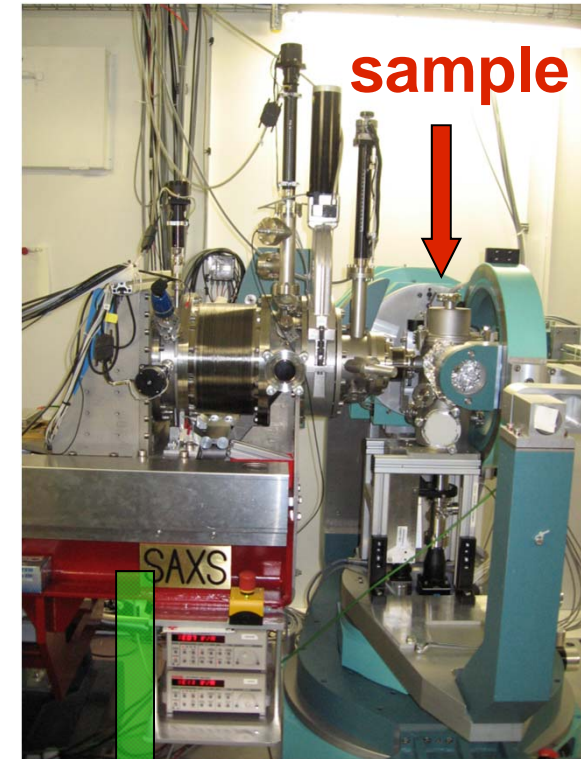
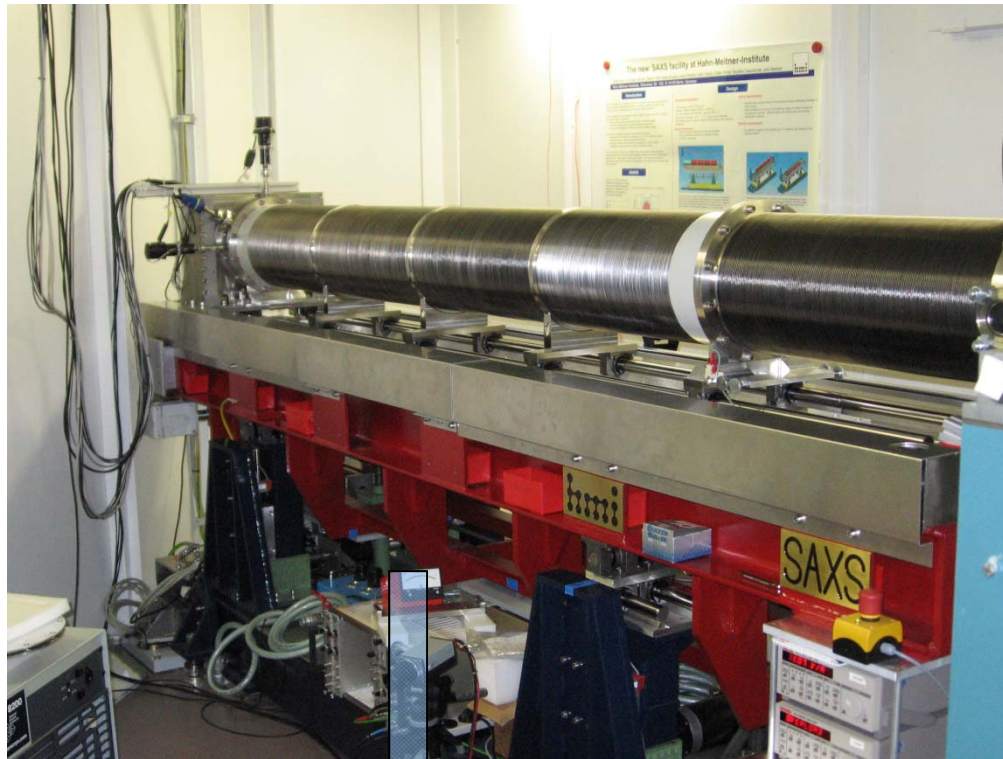
➤ Interferences between the scattering of single particles

Case 4: Sum of two sort of particles with different size distributions

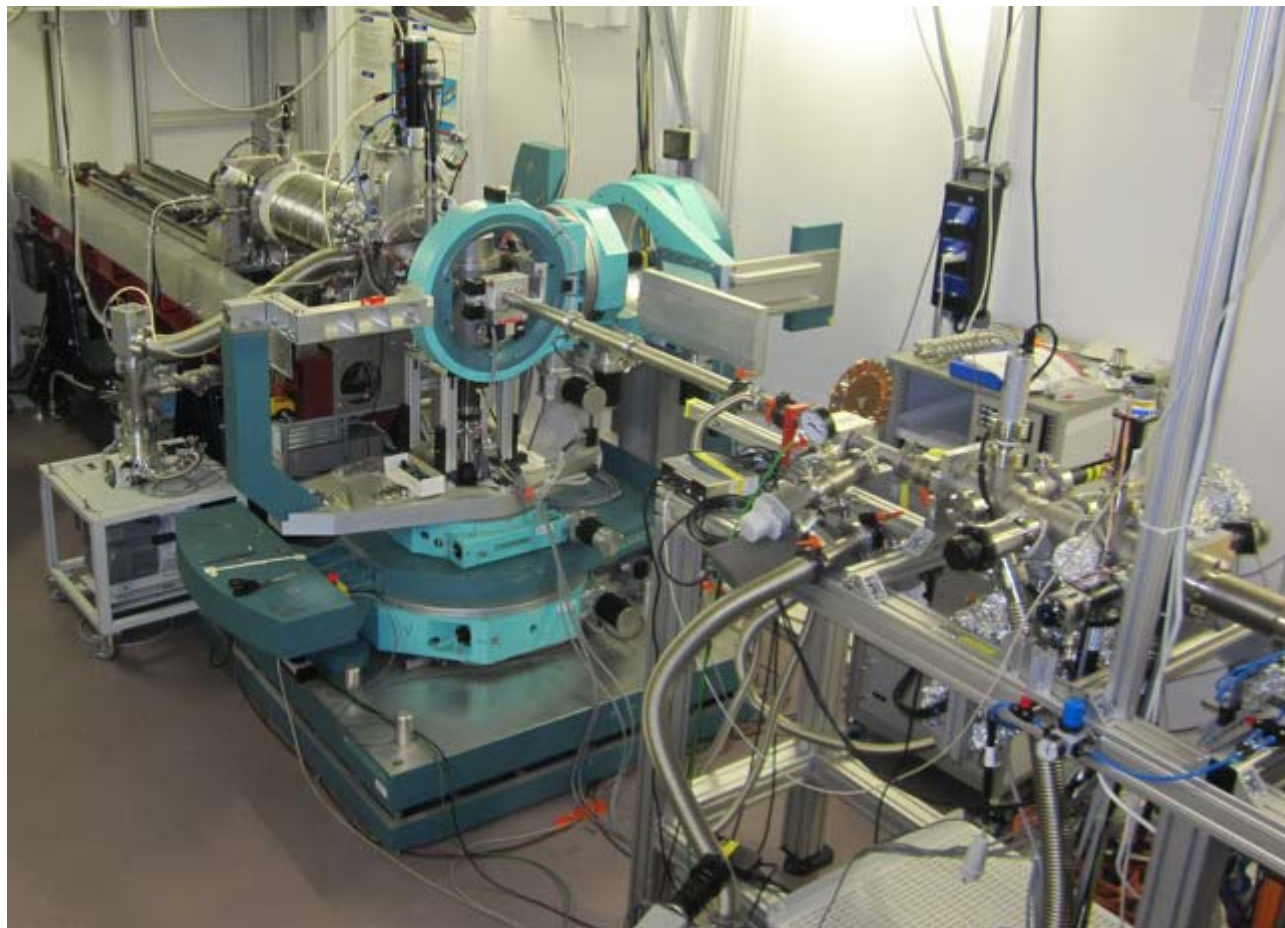


One example of small angle scattering instrumentation

The ASAXS-Instrument at the Synchrotron BESSY II

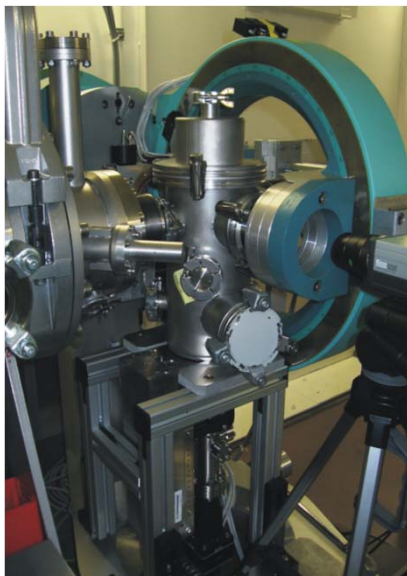


The ASAXS-Instrument from top

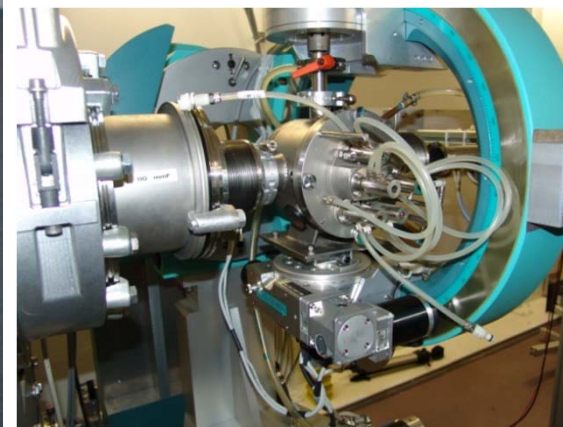


Some sample environments for SAXS

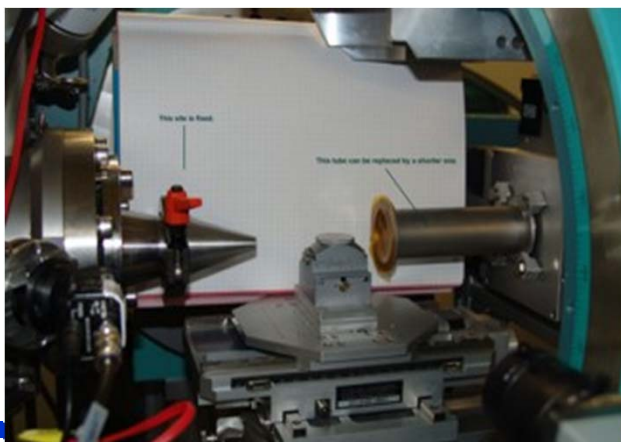
Sample chamber under vacuum

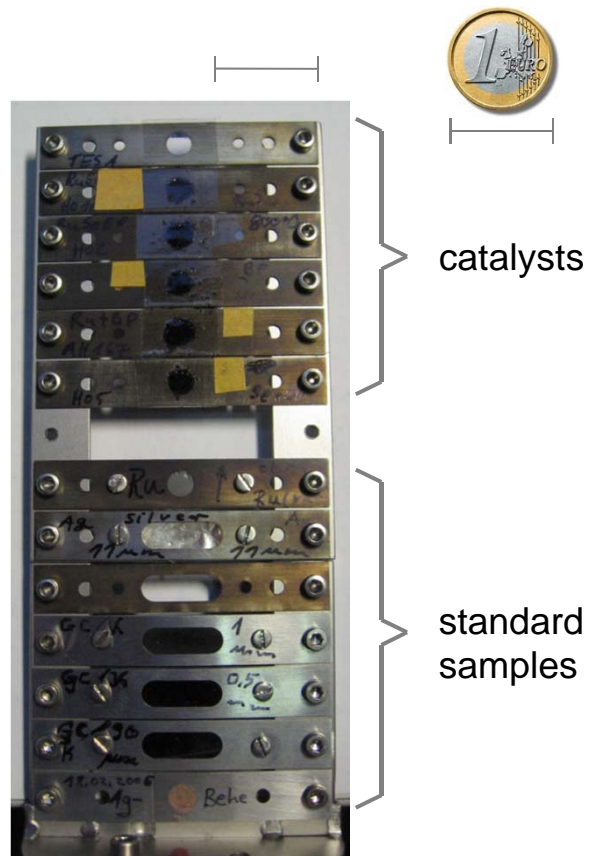


furnaces (293K – 1450K)

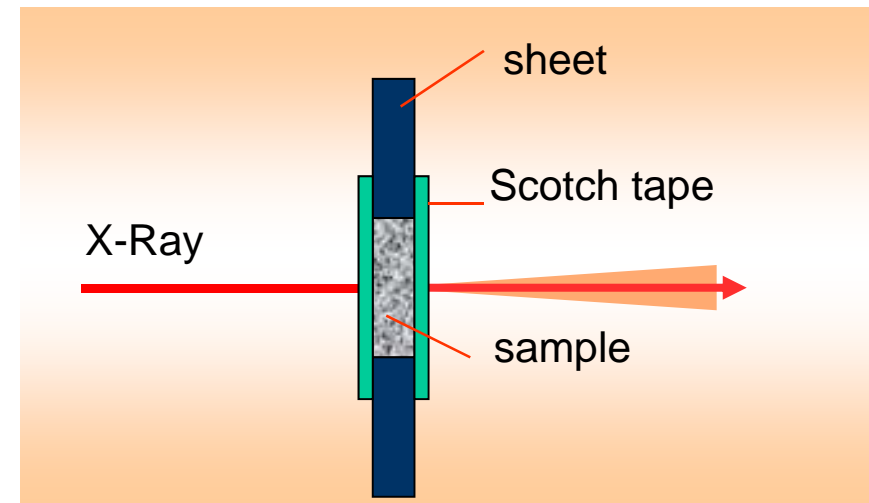


Sample changer on air





Powder samples



Liquid samples



optimal sample thickness:

$$\tau = \exp^{-\mu d} \quad \tau \sim 0.36$$

Why:

more complex systems, mixture of different phases
decide between different structural model solutions

How:

1. Combined use of X-ray and Neutron Small Angle Scattering
2. Isotope substitution in case of neutrons
lack: set of different samples to be prepared
3. Magnetic contrast variation in case of neutrons (polarised N.)
4. Anomalous Small Angle Scattering (ASAXS)
in case of X-rays

X-rays

$$\rho \sum c_i z_i / M_i$$

c_i : composition ρ : density

z_i : electron number

M_i : mass number

Neutrons

nuclear: **magnetic:**

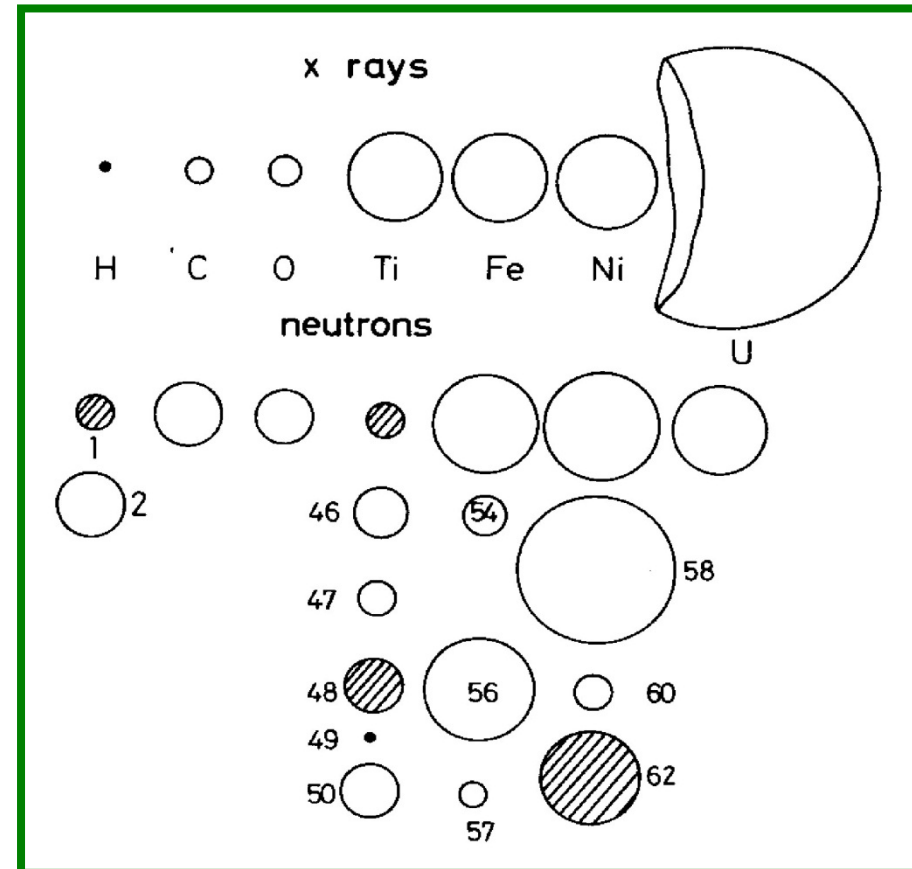
$$\rho \sum c_i b_i$$

$$\rho \sum c_i M_i^\perp$$

b_i : scattering

M_i^\perp : magnetization

length



-radii of the circles are proportional to the scattering length
-negative values are indicated by cross-hatched shading

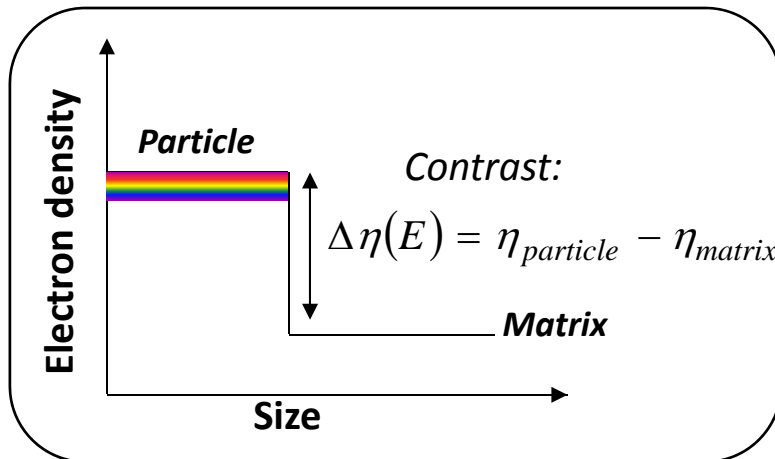
➤ Scattering Intensity

$$I(q, E) = \int_0^\infty N(r) V_p(r)^2 |F(q, r, \Delta\eta(E))|^2 S(q, r) dr$$

Size distribution
Volume
Form factor
Structure factor

- Sc. Amplitude for a homogenous sphere of radius R:

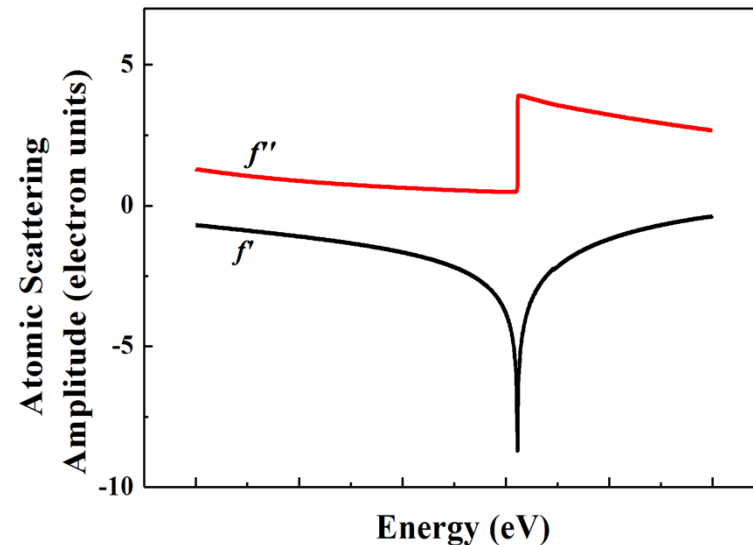
$$F(q, R, \Delta\eta(E)) = \Delta\eta(E) 3 \frac{\sin(qR) - (qR) \cos(qR)}{(qR)^3}$$



effective electron density

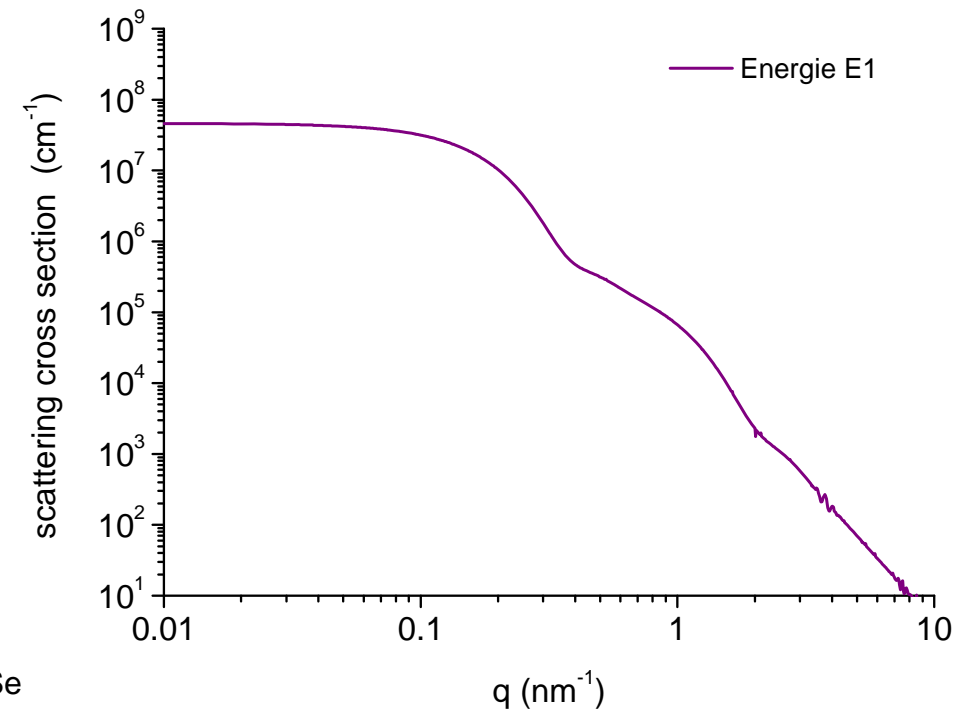
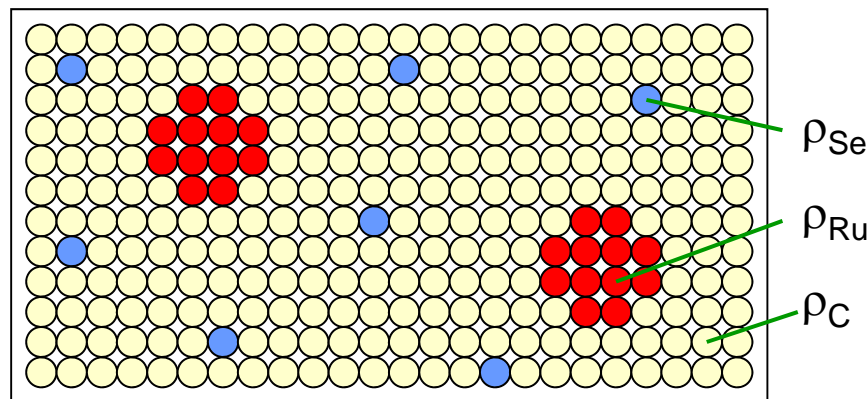
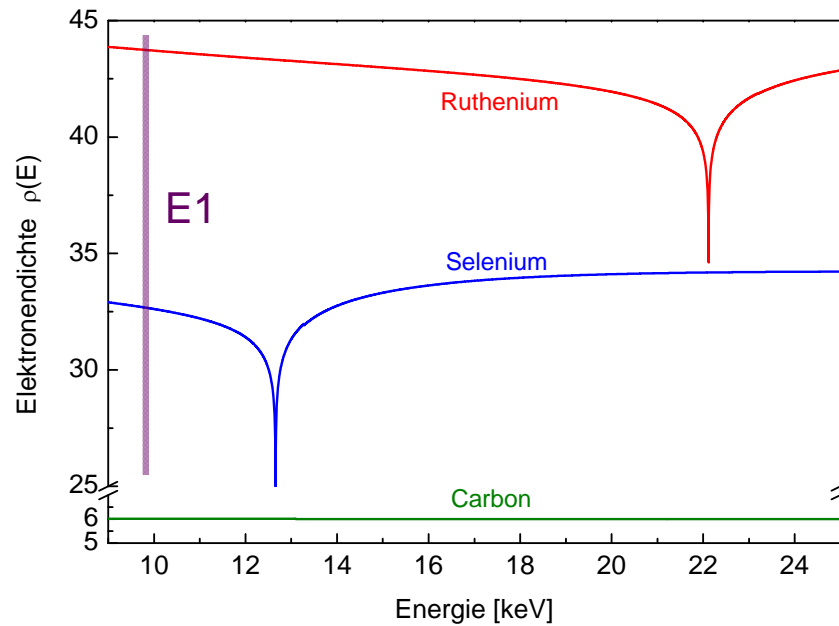
$$\eta(E) = \frac{N_A D \sum c_i f_i(E)}{M_C}$$

$$f(E) = f_0 + f'(E) + if''(E)$$

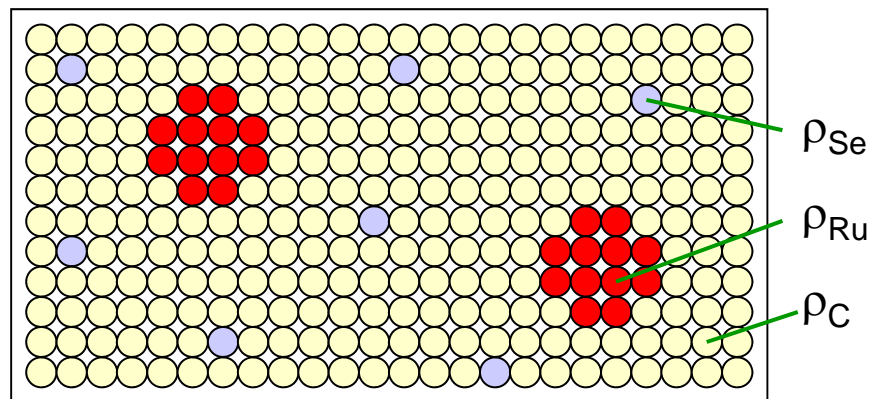
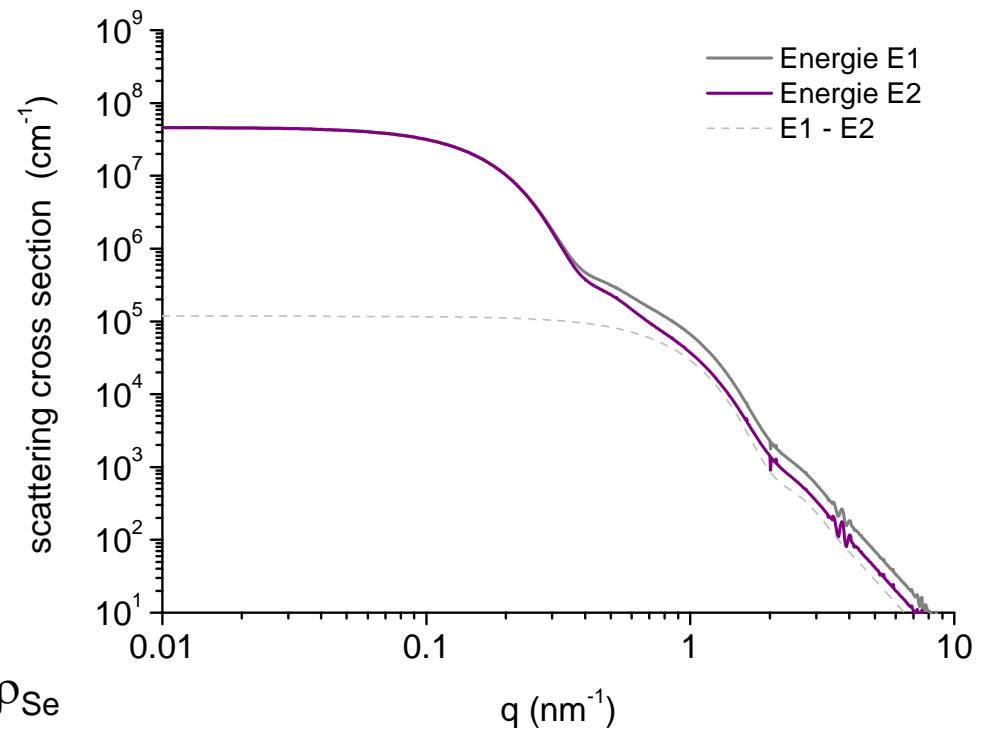
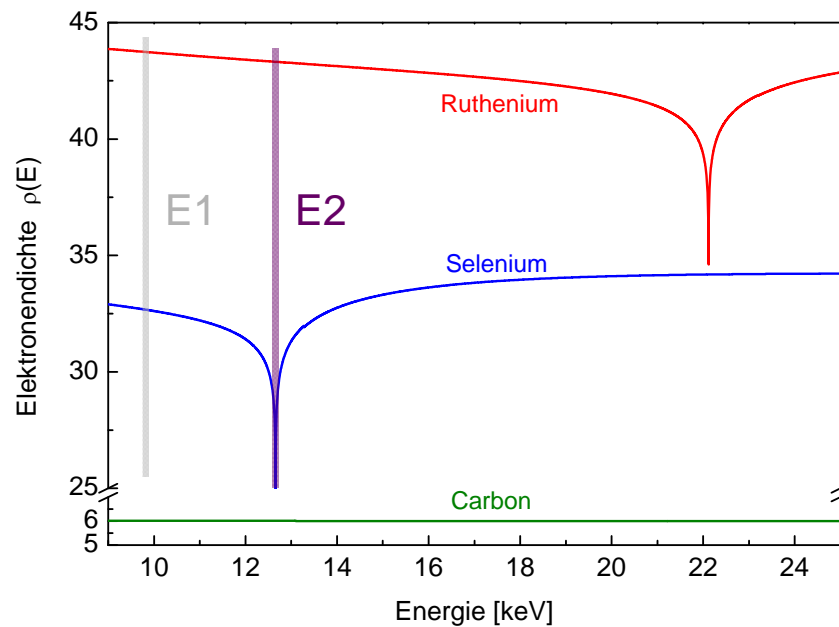


- ASAXS: Energy dependency of the atomic scattering amplitudes

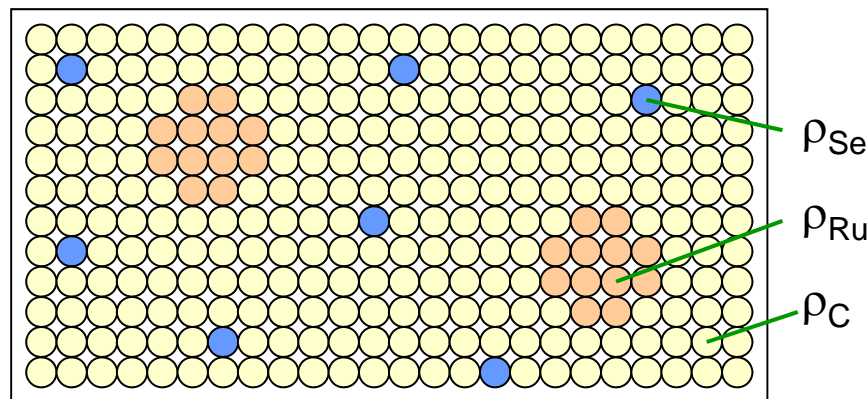
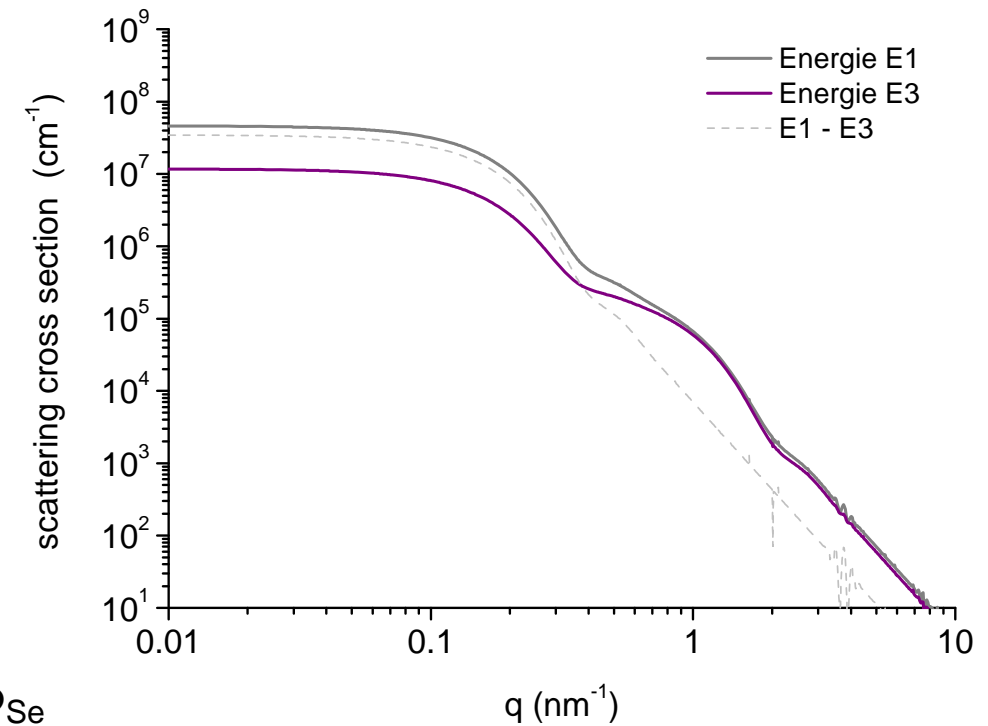
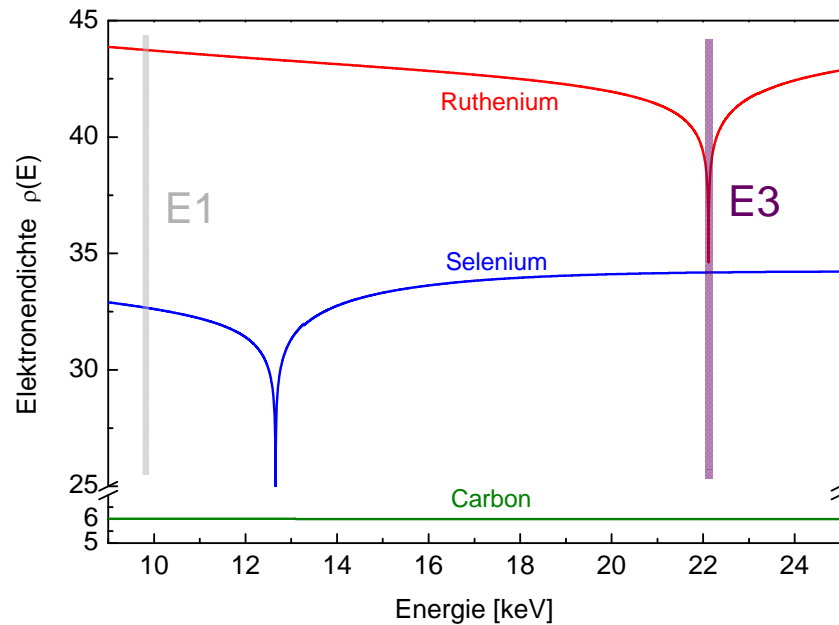
- effective “electron density” becomes energy dependent.

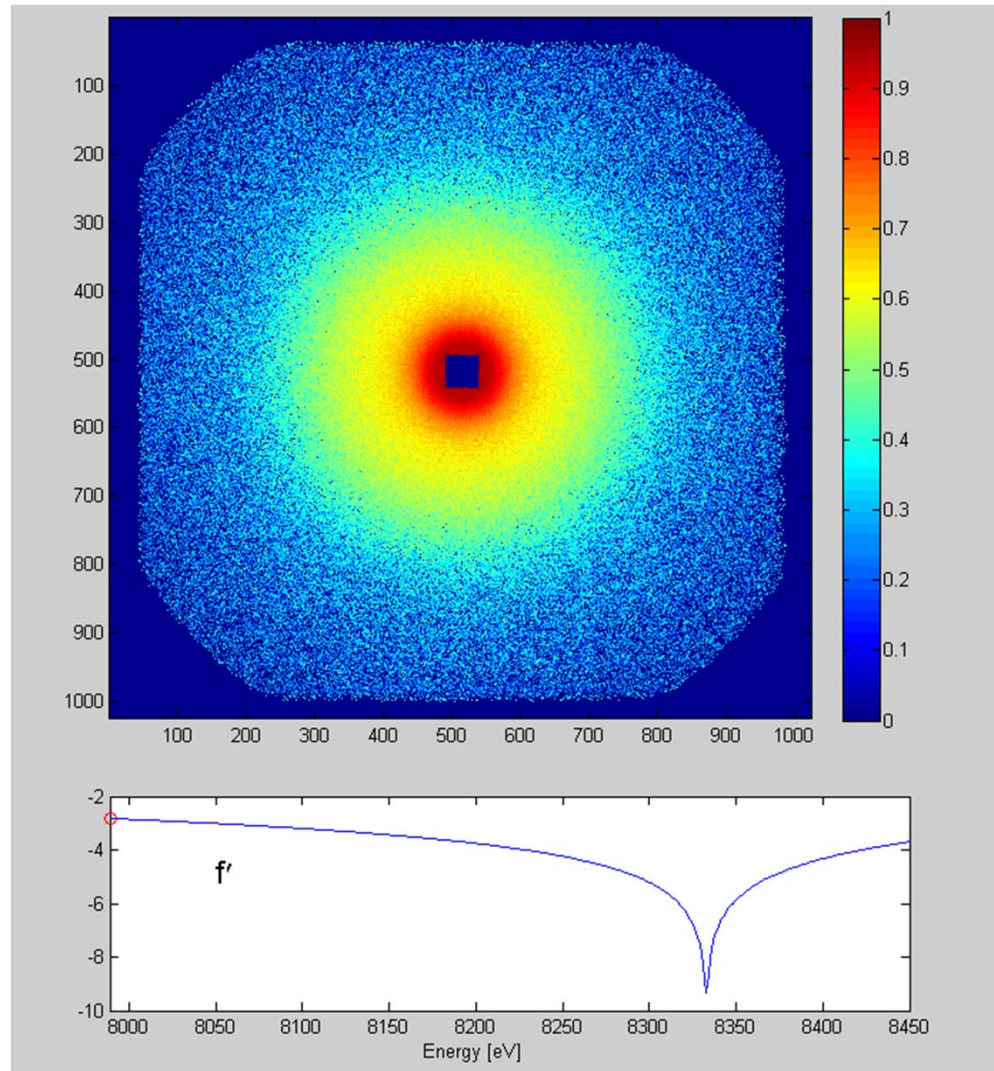


➤ effective “electron density” becomes energy dependent.



- effective “electron density” becomes energy dependent.



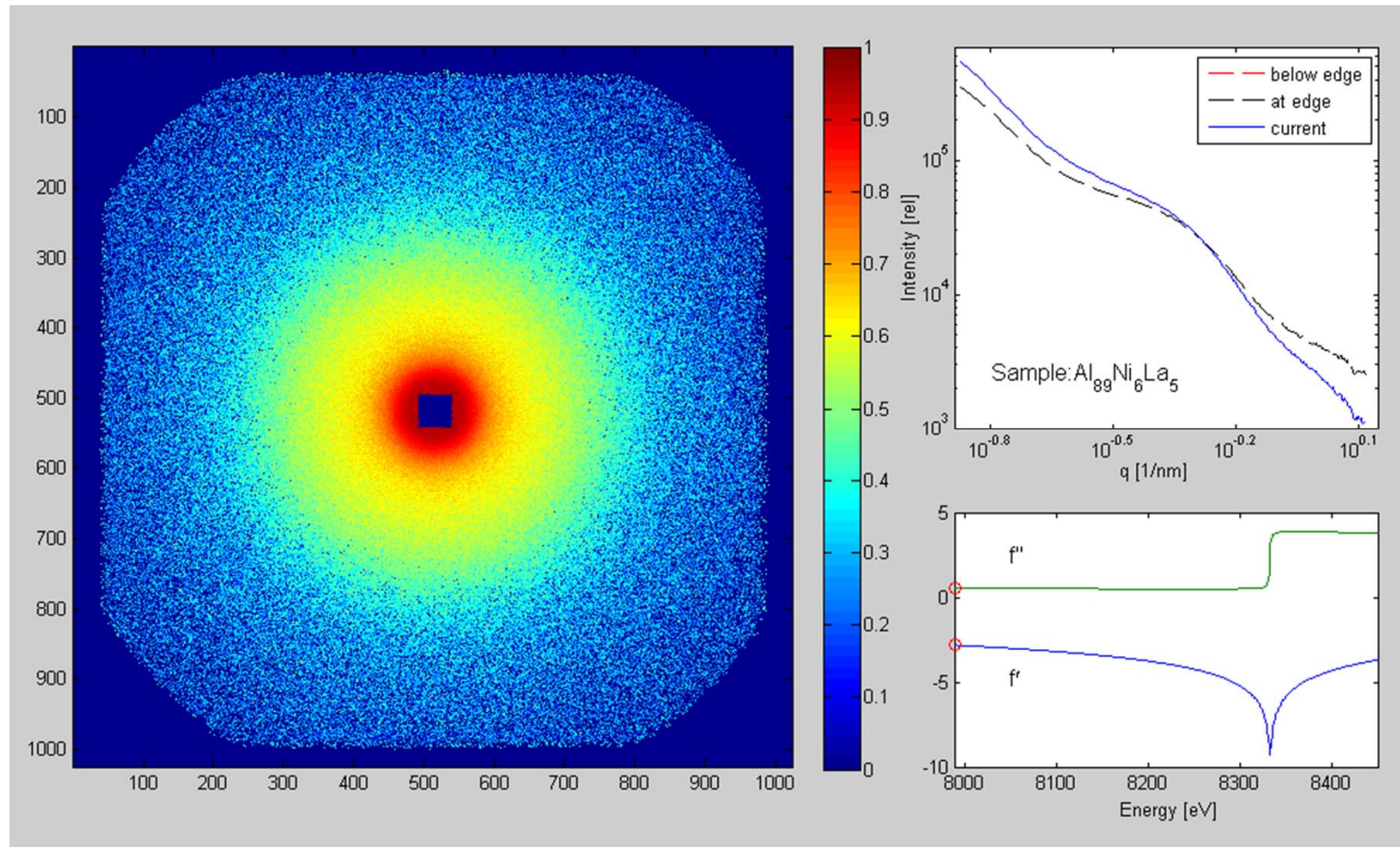


- measured:
- 8000eV – 8450eV
 - $\Delta E = 2.25\text{eV}$
 - 201 energy steps
 - constant q -range on 2D gas detector

2D gas detector:

corrected by deadtime, monitor, transmission, detector sensitivity, solid angle distortion, projection of detector surface on a sphere, and background subtraction

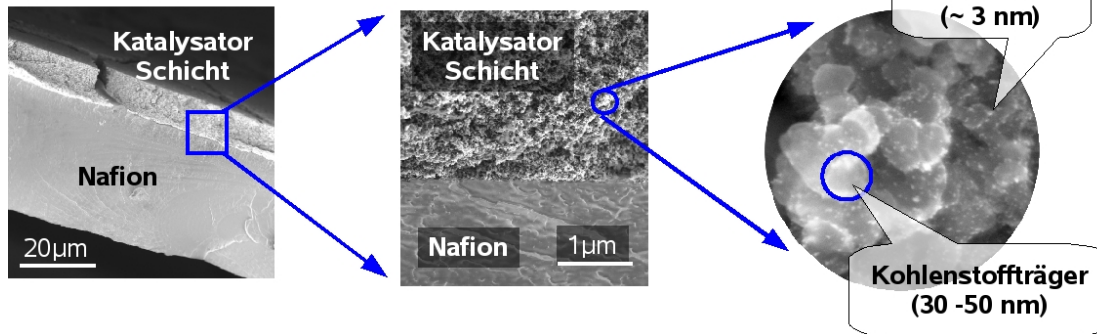
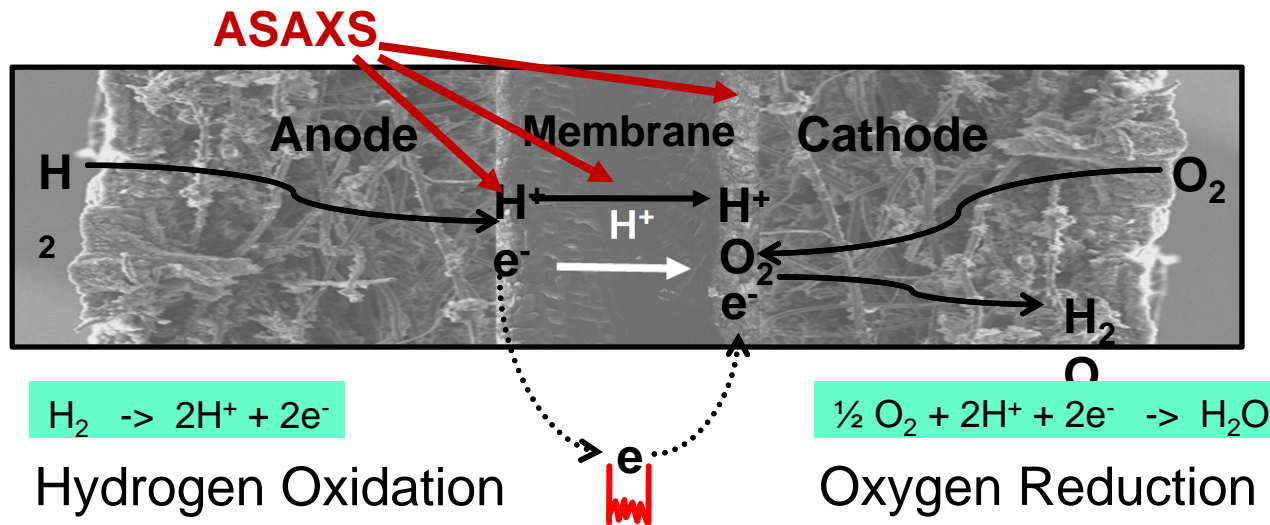
Instrument: SAXS @ BESSY



scattering curves are extracted from the corrected 2-dim. detector pictures

Example 1: RuSe Nanoparticle for fuel cell applications

Example 2: In situ study of the degradation of PtNi₃ alloys



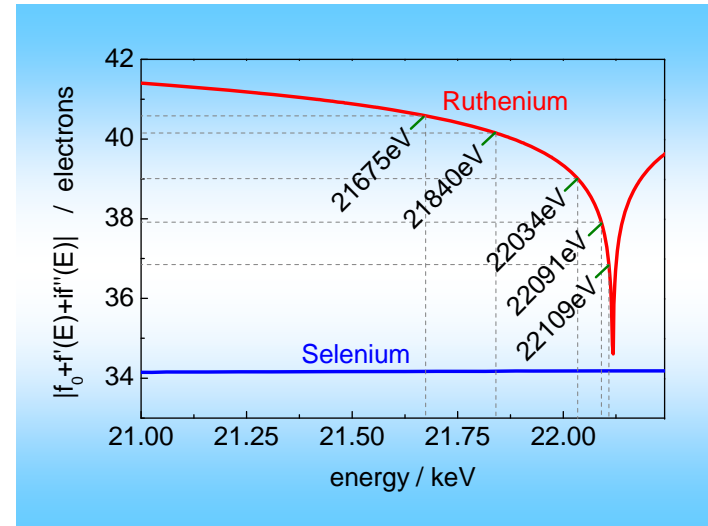
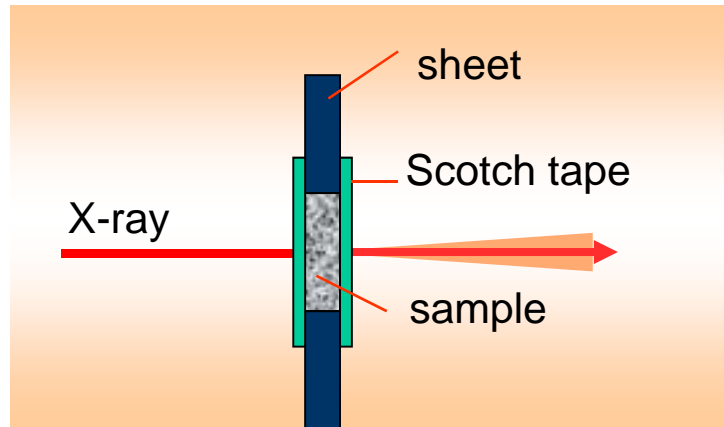
Ru-Se Catalyst for fuel cells

Slow electrode kinetics,
Cost of catalyst,
Catalyst degradation...

...are the most critical issues in fuel cell research

$$f(E) = f_0 + f'(E) + if''(E)$$

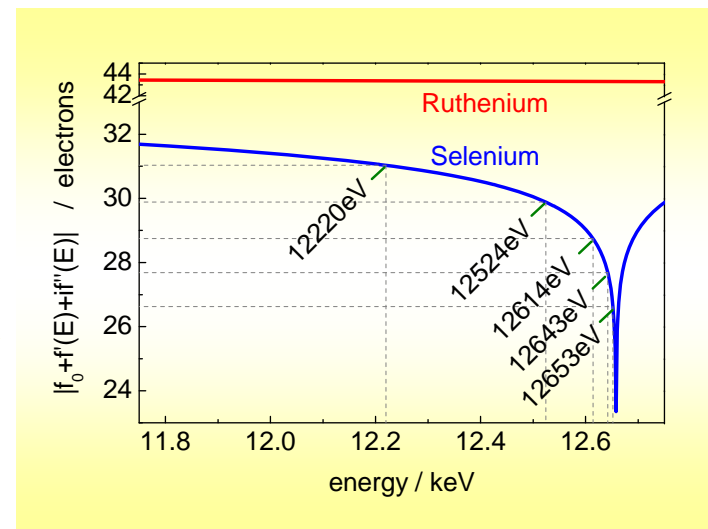
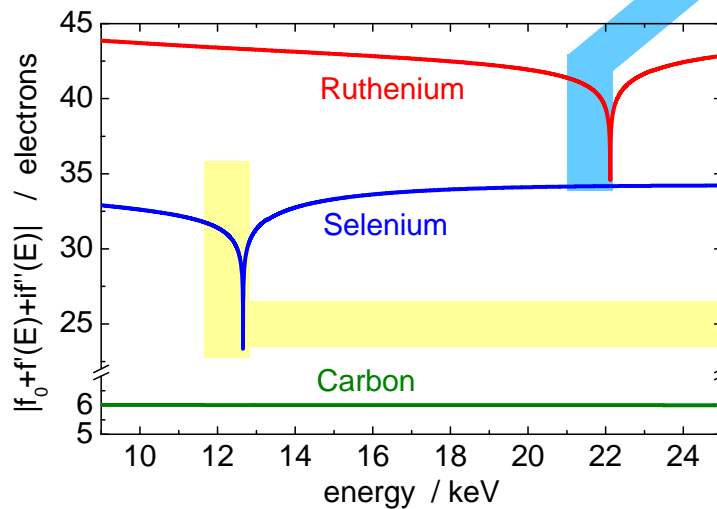
Sample preparation



Ru K edge

- 442 eV
- 277 eV
- 83 eV
- 26 eV
- 8 eV

Atomic scattering amplitudes



Se K edge

- 438 eV
- 134 eV
- 44 eV
- 15 eV
- 5 eV

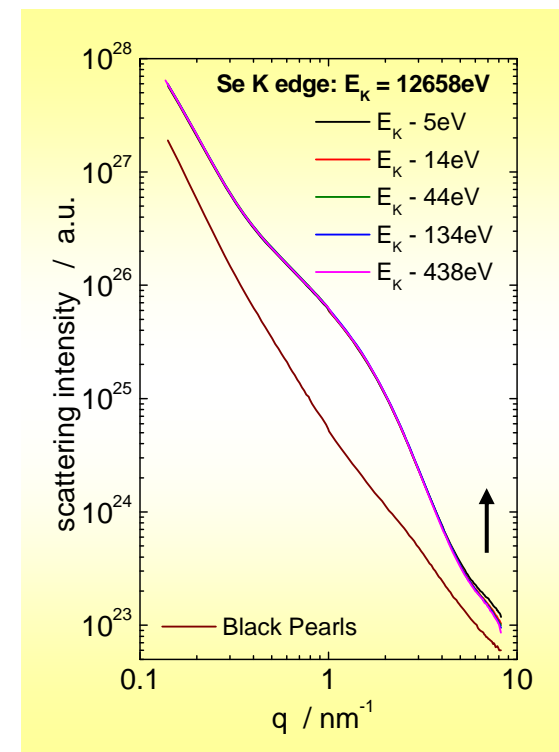
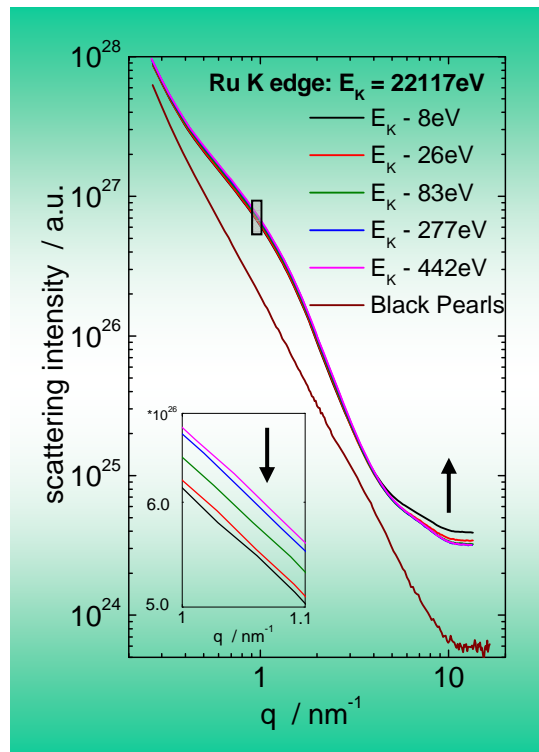
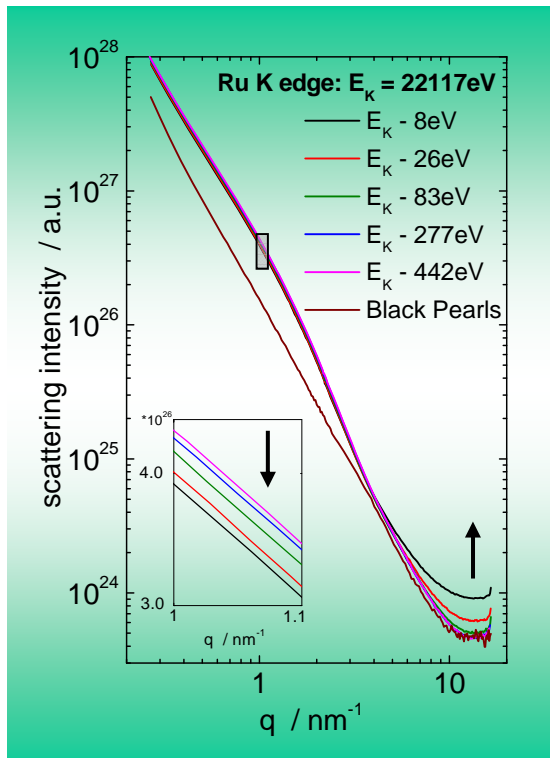
Ru-K-edge (22117eV)

Se-K-edge (12658eV)

Ru on Black Pearls

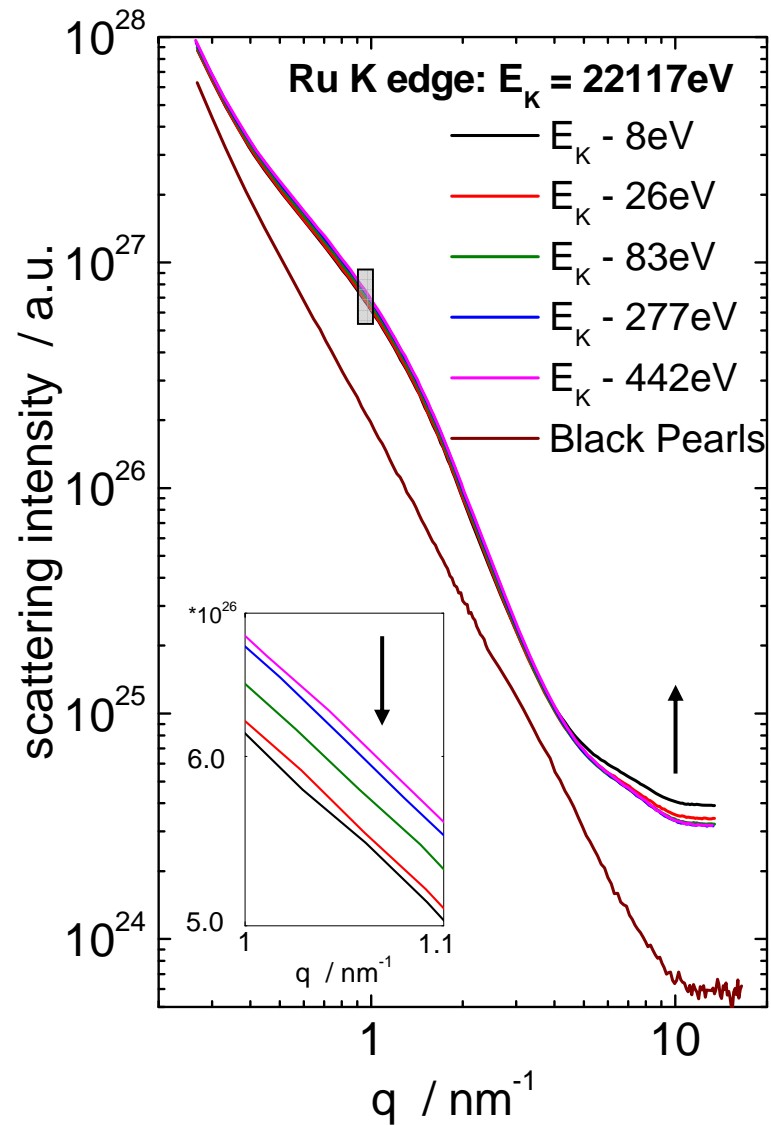
RuSe_x on Black Pearls

RuSe_x on Black Pearls

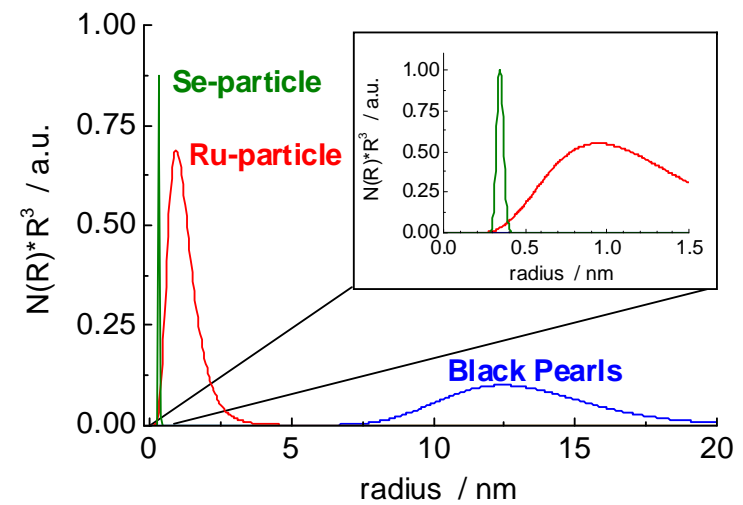


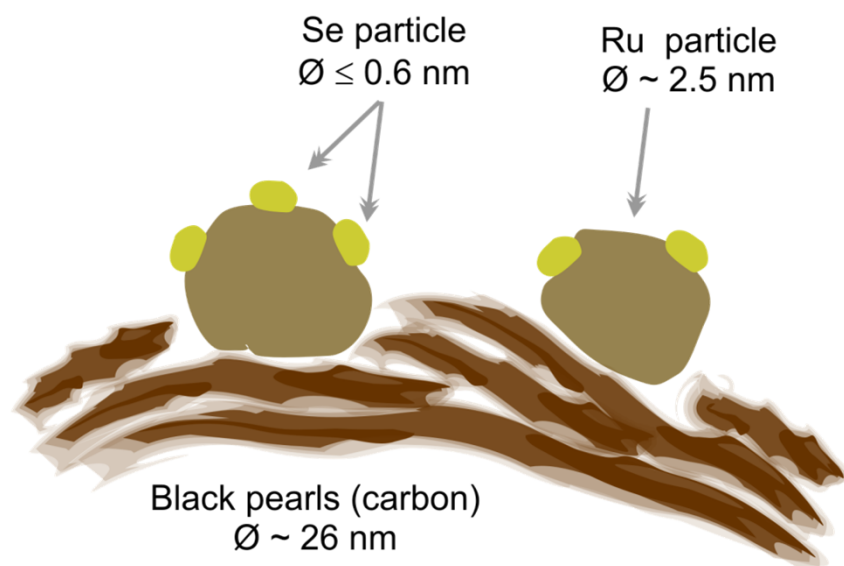
→ clear anomalous effect

→ no anomalous effect

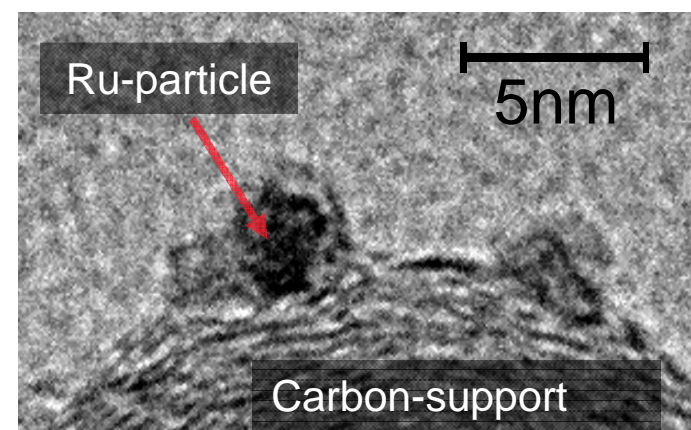


Volume weighted size distribution





TEM



G. Zehl, G. Schmithals, A. Hoell, S. Haas, C. Hartnig, I. Dorbandt, P. Bogdanoff, and S. Fiechter, *Angew. Chem. Int. Ed.* 2007, **46**, 7311–7314

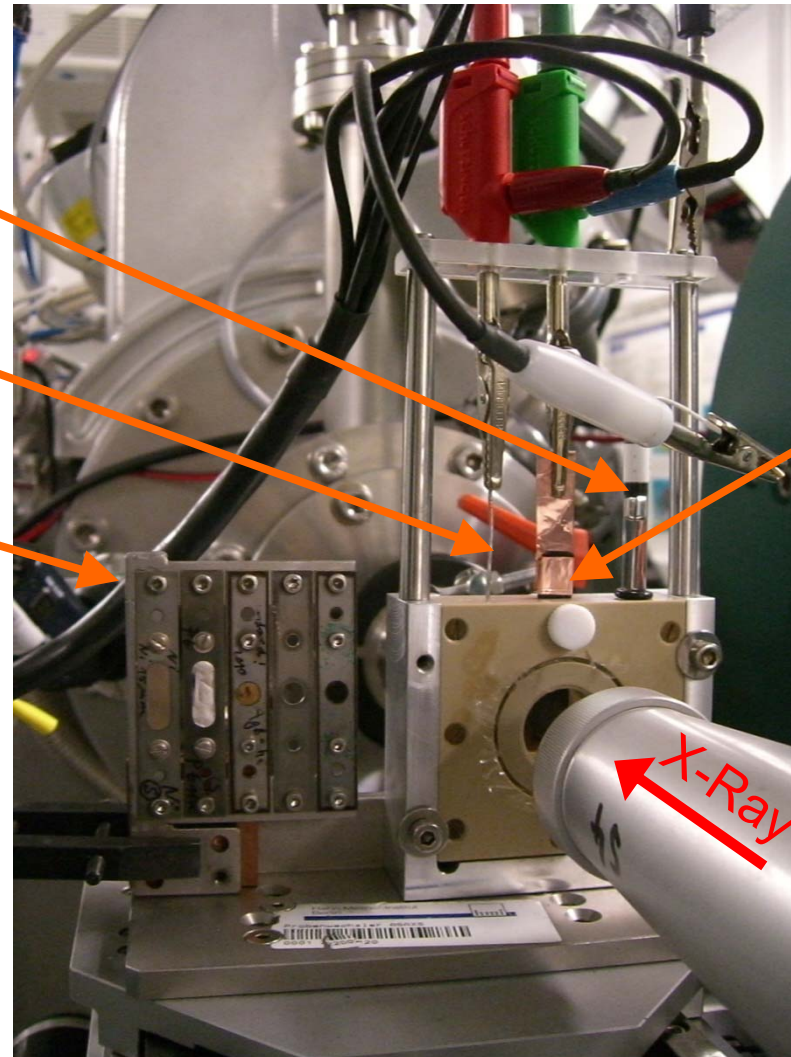
Example 1: RuSe Nanoparticle for fuel cell applications

Example 2: In situ study of the degradation of PtNi₃ alloys

Reference
electrode

Counter
electrode

Reference
samples
for ASAXS



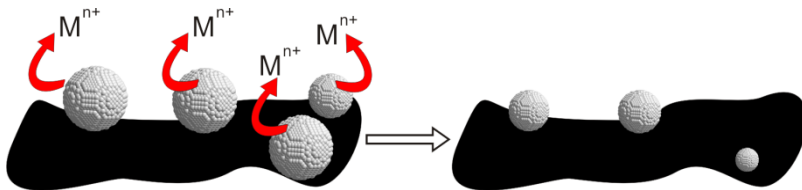
Working
electrode



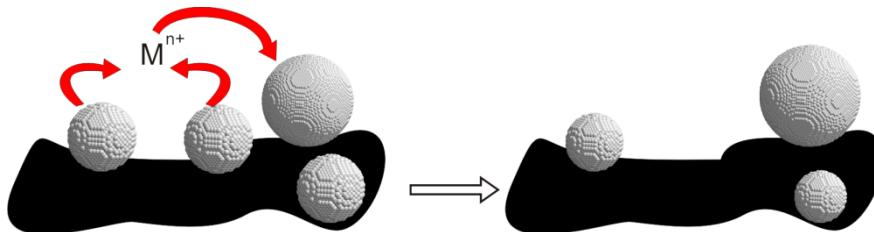
Catalyst ink
droplet

SAXS is capable to distinguish the mechanism of particle surface area loss

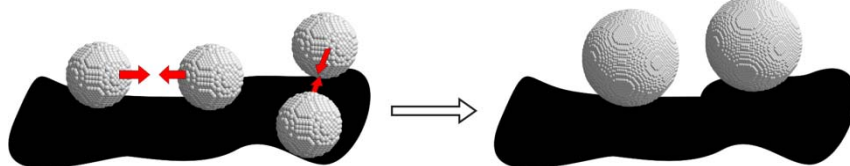
1. Dissolution



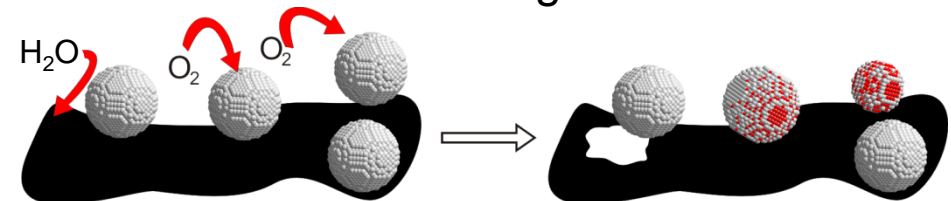
2. Ostwald Ripening



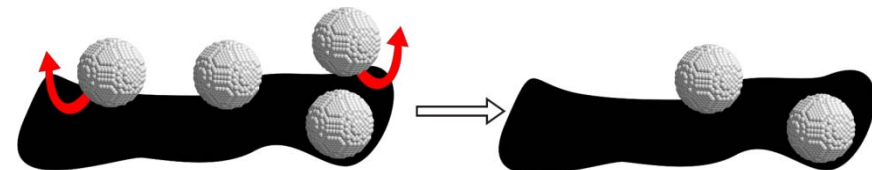
3. Coalescence



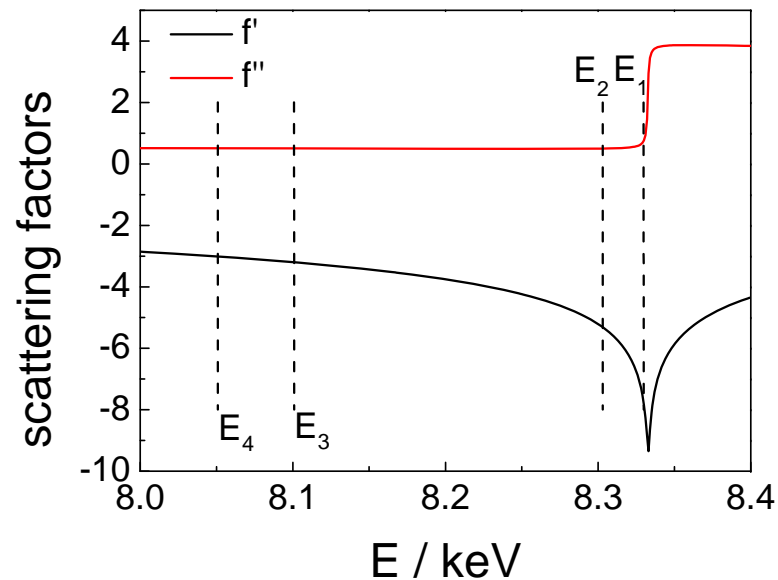
4. Oxidation/Poisoning



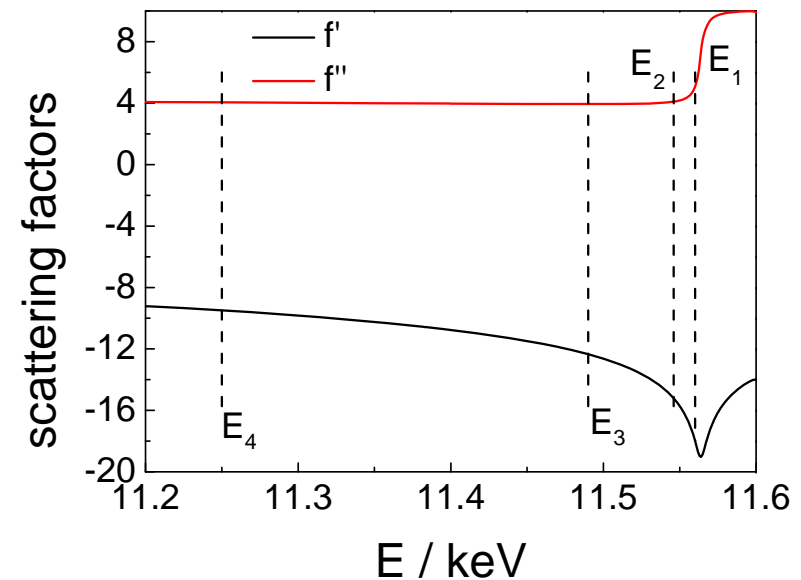
5. Mechanical detachment from conductive support



For Ni-resonant scattering



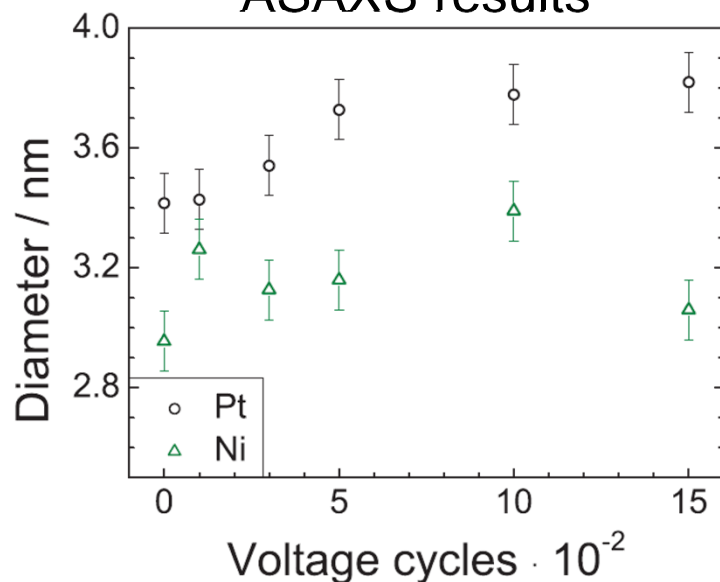
For Pt-resonant scattering



The protocol was kept the same as for the electrochemical characterization.

ASAXS was monitored during a chronoamperometry at 0.5 V after a certain number of stress cycles (0.5 – 1.1 V)

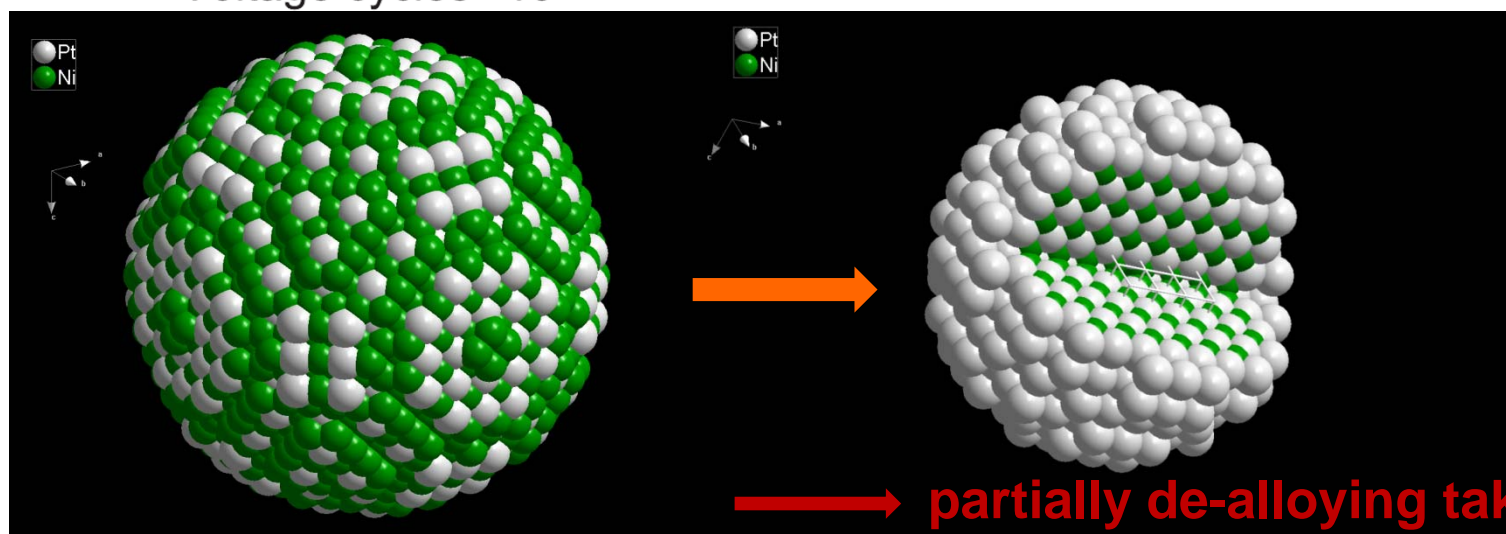
ASAXS results

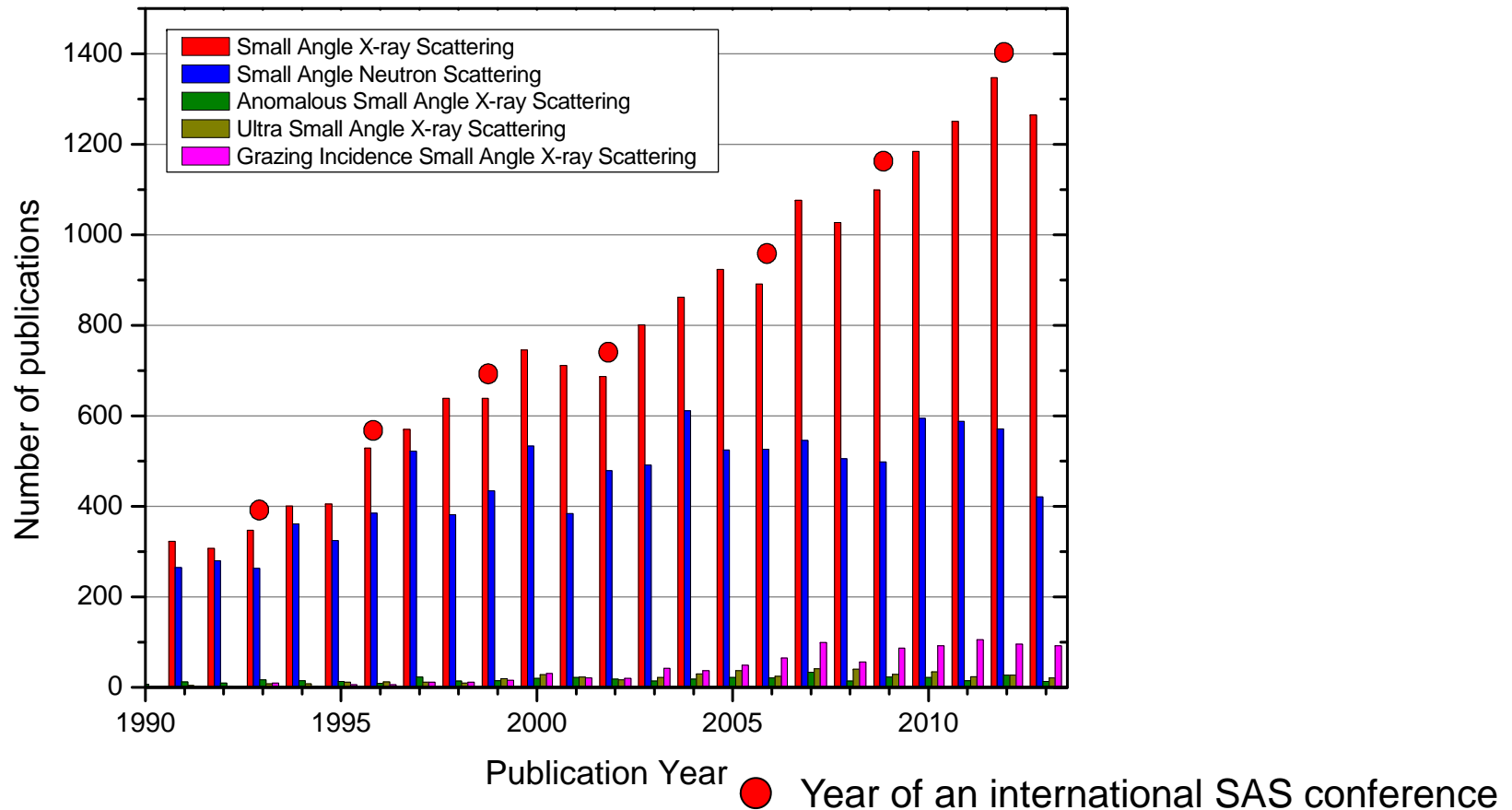


HE-XRD: PDF-analysis

Pristine particles: partially chemically ordered PtNi₃ single phase.

Stressed particles: predominant PtNi₃ phase and Ni phases.

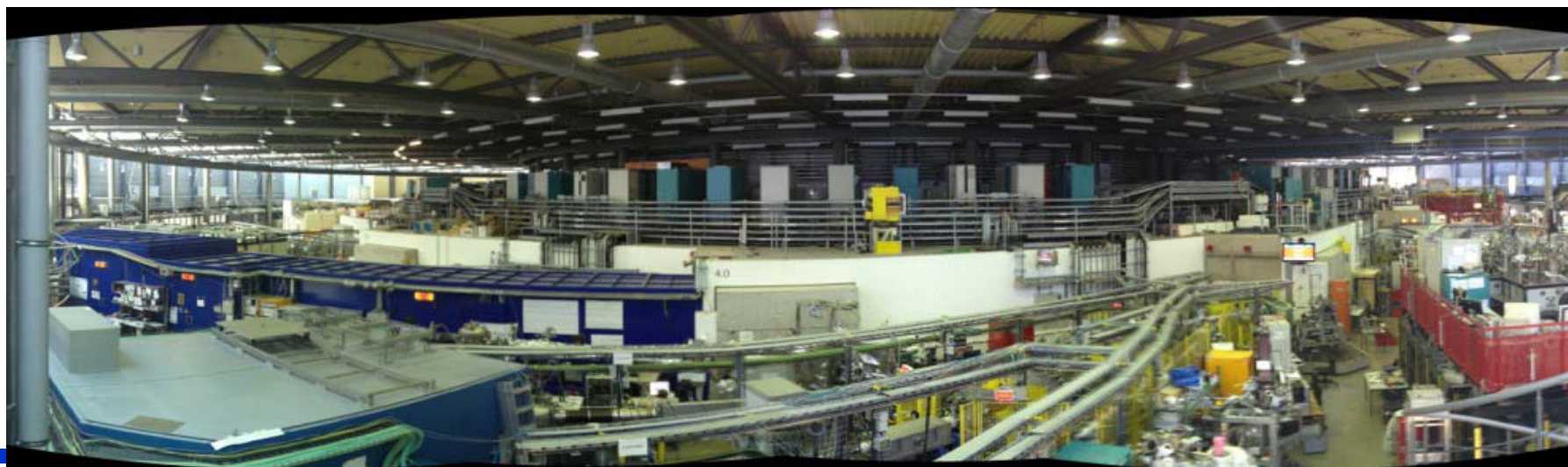




Next international Conference on Small-Angle Scattering:
13. – 18. September 2015, TU Berlin (about 500 participants expected)



Thank You!



Lecture: Introduction to Small-Angle Scattering: FHI Berlin WS 2014-2015